

Review

# Review of Photogrammetric and Lidar Applications of UAV

Ľudovít Kovanič <sup>1,\*</sup>, Branislav Topitzer <sup>1</sup>, Patrik Peťovský <sup>1</sup>, Peter Blišťan <sup>1</sup>,  
Marcela Bindzárová Gergeľová <sup>1</sup> and Monika Blišťanová <sup>2</sup>

<sup>1</sup> Institute of Geodesy, Cartography and Geographical Information Systems, Faculty of Mining, Ecology, Process Control and Geotechnologies, Technical University of Kosice, Park Komenského 19, 04001 Košice, Slovakia

<sup>2</sup> Faculty of Aeronautics, Technical University of Kosice, 04001 Košice, Slovakia

\* Correspondence: ludovit.kovanic@tuke.sk

**Abstract:** Using Unmanned Aerial Vehicles (UAVs) combined with various sensors brings the benefits associated with fast, automatic, and contactless spatial data collection with high resolution and accuracy. The most frequent application is the possibility of effectively creating spatial models based on photogrammetric and lidar data. This review analyzes the current possibilities of UAVs. It provides an overview of the current state of the art and research on selected parameters regarding their history and development, classification, regulation, and application in surveying with creating spatial models. Classification and regulation are based on national sources. The importance and usability of this review are also carried out by analyzing the UAV application with selected photogrammetric and lidar sensors. The study explores and discusses results achieved by many authors in recent years, synthesizing essential facts. By analyzing the network of co-occurring High-Frequency Words, in addition, we visualized the importance of the primary keyword UAV in the context of other keywords in the literary sources processed.

**Keywords:** UAV; photogrammetry; lidar; point cloud; SfM; DSM; DEM



**Citation:** Kovanič, Ľ.; Topitzer, B.; Peťovský, P.; Blišťan, P.; Gergeľová, M.B.; Blišťanová, M. Review of Photogrammetric and Lidar Applications of UAV. *Appl. Sci.* **2023**, *13*, 6732. <https://doi.org/10.3390/app13116732>

Academic Editors: Andrea L. Rizzo, Na Zhao and Hua Zhong

Received: 26 February 2023

Revised: 29 May 2023

Accepted: 29 May 2023

Published: 31 May 2023



**Copyright:** © 2023 by the authors. Licensee MDPI, Basel, Switzerland. This article is an open access article distributed under the terms and conditions of the Creative Commons Attribution (CC BY) license (<https://creativecommons.org/licenses/by/4.0/>).

## 1. Introduction

In recent years, mapping and surveying the landscape, terrain, and the Earth's surface have been the most dynamic, efficient, and progressive surveyor tasks. They made significant progress thanks to the development of technology and software equipment. Non-contact methods are preferably used to map the landscape, including radar scanning, laser scanning, or aerial and terrestrial photogrammetry. Non-contact methods provide a large amount of spatial data with high accuracy and detail, which capture parts, elements, and components of the landscape or the Earth's surface. The most common outputs from data collection using non-contact methods are aerial images, digital terrain and surface models, point clouds, vector maps, and orthophoto maps representing real-world objects [1,2].

Among non-contact methods, laser scanning is increasingly used for landscape and terrain mapping. Laser scanning is an active method of remote exploration of the Earth, which uses electromagnetic radiation as a source. Laser scanning enables the recording of the 3D geometry of objects, surfaces, and landscape relief with high accuracy and detail in a relatively short time [3–6]. Another non-contact method of data collection in the field is photogrammetry. Structure from Motion (SfM) reconstruction is a modern and advanced method in the photogrammetric processing of images [7–9]. The main principle of the SfM method is to estimate the three-dimensional structure of a spatial object using two-dimensional images resulting from a moving recording media carrier (digital camera, video camera). The main advantage of the SfM method is its availability and deployment in practice with precise and detailed results.

Using non-contact methods based on piloted or the more available remotely piloted (unmanned) aerial vehicles is currently very popular. We distinguish between piloted

(planes, helicopters, balloons, airships) and remotely piloted (UAV, UAS, RPAS) airborne carriers. Today, UAVs are preferred because they are affordable and easy to use. Their advantage is in minimizing fieldwork, applying the high speed of photogrammetric data collection, and processing with a high level of detail and accuracy of results. As a result, UAVs are currently used in almost every scientific, technical, and non-technical discipline.

A global navigation satellite system (GNSS) defines the sensor's orientation and position. It locates the geographical position of the sensor, along with the Inertial Measurement Unit (IMU), which measures the aircraft's speed, pitch, orientation, and exact position [10].

When choosing a data-collection method, area size, required density of points, positional and height accuracy, the time needed for fieldwork, and economic aspects must be considered. The accuracy of the resulting model depends on camera parameters, the accuracy of measurement of image coordinates, image configuration, defining the coordinate system, the accuracy of the scale and ground control points (GCP), quality of camera calibration, the stability of internal orientation elements, and other parameters. In surveying applications, the use of GCP points is required to verify the accuracy of measurements. GCPs are used for georeferencing photogrammetric data. With the help of GCPs, the internal and external orientation elements on the images are correctly determined. Determining GCP coordinates requires the use of classic geodetic methods with subsequent transformation into positional and height coordinate systems. The second option is to use the RTK/PPK approach position when imaging. Then, each image is assigned a precise position. In this case, GCPs are not necessary but are recommended. This alternative is mainly used when stabilizing GCP points in the field is difficult. Many authors [11–15] have investigated and compared the accuracy of UAVs with onboard RTK/PPK GNSS versus UAV measurement using GCP points with relevant and interesting results. However, using a UAV with an onboard GNSS RTK revealed less accuracy in the vertical component of the resulting model or systematic elevation error. This inaccuracy can be improved by adding only a few GCPs or combining multiple flights.

This article's main contribution is summarising and expanding our knowledge on applications using UAVs. We focused on analyzing the results achieved by different UAVs and different sensors and in different areas of their application. This contribution is based on a comprehensive review of the scientific literature. The primary source for the literature overview was the Web of Science database, followed by Scopus and Google Scholar databases using their search engines. The main keyword in the search was "UAV", along with alternatives such as "UAS", "RPAS", and "drone". Additional keywords in the search were products of UAV missions such as point cloud, DEM, DTM, etc., and the field of application of UAV such as surveying and mapping, industry, archeology, etc.

Separate keywords associated with the main keyword UAV formed the basis for the analysis of co-occurrence, which we present in a processed network of co-occurring high-frequency words. This search yielded a sample of 213 records. This part of the study is mainly focused on the co-occurrence method to analyze articles from various indexed journals obtained for 2013–2022. The most frequently occurring words express and identify the relationship between other conceptual sub-subjects with which they are associated. The open-source VOSviewer (<https://www.vosviewer.com/>, accessed on 1 January 2023) was used to analyze and visualize the obtained results. As a result, our literature review can save time for readers of this topic to quickly find and understand the content and orientation of the literature on the subject of UAVs in combination with several sensors, mainly in the field of spatial data collection.

## 2. History of UAV

According to the literature [16], UAV remote sensing applications and techniques have come a long way and are based on almost 150 years of unmanned remote sensing with different types of sensors and platforms. Kites, balloons, airships, paragliders, model airplanes, and helicopters were the most common platforms used before modern aircraft. The first experiments with cameras attached to kites and balloons were carried out in

the mid-19th century by the French engineer Colonel Aimé Laussedat, who was later considered the father of photogrammetry. More successful attempts at unmanned aerial photography using balloons were made in the 1860s and 1980s in America, Germany, and France. Until the beginning of the 21st century, the kite was the most widespread unmanned platform for obtaining images from low altitudes. The successful use of the kite as a platform for scientific measurements is documented in the publications of British and American meteorologists [17,18]. After the invention of powered airplanes by the Wright brothers at the turn of the 19th and 20th centuries, the role of kites and balloons declined as more aerial photographs were taken from planes. Technical developments in the field of cameras, film, and photo analysis were rapidly developed during the First World War and again during the Second World War due to the need for military surveying and accurate cartographic measurement and mapping. After World War II, photographic equipment and aerial photographs became available in non-military fields and scientific applications. The development of satellite remote sensing during the Cold War pushed Earth observation into new areas again, with unmanned platforms at orbital heights outside airspace. Later, digital scanning sensors provide a new type of imagery. However, the processing of satellite images was very demanding and was carried out by trained specialists with access to specialized and expensive hardware and software. Therefore, at the same time, in the 1970s and 1980s, in addition to satellite remote sensing, low-altitude aerial photography using a platform and sensors with cheap and accessible technology made significant progress, which formed the basis for the discipline of UAV remote sensing that we know today.

### 3. Classification of UAV

In general, UAVs can be classified according to various parameters. Nowadays, there are already a large number of UAVs, which are specific in terms of their construction and parameters, weight, size, height, or range reach. The manufacturers of these technologies can adapt the UAV directly for the given purpose. For this reason, it is not easy to classify UAVs into individual categories; in general, there is no uniform classification standard in this industry. Many characteristics of these devices influence each other, which affects their flight and user characteristics. The European Union Aviation Safety Agency (EASA) has created a system for categorizing unmanned vehicles, which divides them according to several factors. European UAV legislation distinguishes three basic categories of UAVs according to the method of use and the level of risk—Open, Specific, and Certified. The category Specific includes UAV operations with a higher degree of risk and primarily concerns professional pilots of unmanned devices. UAVs are specified here based not on parameters but on how they are used. The category Certified corresponds to operations with the highest level of risk. In the future, UAV flights with passengers on board will fall here. The open category includes the use of UAVs up to 25 kg for recreational purposes and commercial activities with a low level of risk. Most UAV users fall into this category. This category is subsequently divided according to the maximum flight weight of the UAV into subcategories A1, A2, and A3, as shown in Table 1. When a UAV is used for commercial purposes, then UAV is classified in category B. The pilot needs a license to perform aerial works, which will be obtained after passing theoretical and practical tests. Submitting the operating manual, insurance, and registration of the UAV at the Transport Office is mandatory. This process takes several months, but it is justified. This classification was valid until 31 December 2022. Suppose the user acquires a UAV after 1 January 2023. In that case, the UAVs will be divided into classes C0 to C6, based on technical parameters. A class should be marked by a label from the manufacturers [19,20].

**Table 1.** UAV classification by purpose of use and weight.

Category	Subcategory	Class	Weight
A	A1	C0	<250 g
		C1	250 g–900 g
	A2	C2	900 g–4 kg
	A3	C3 C4	4 kg–25 kg
B		C0–C4	0–25 kg >25 kg

In this case, we classified UAVs according to size, range and endurance, weight, wingspan, the number of rotors, and the purpose of use.

### 3.1. Based on the Size

Size is often a main factor in deciding which UAV is right for the mission. For this reason, it is also one of the main ways of categorizing UAVs. According to the [21], classification according to size can be divided into the following subclasses, which is shown in Table 2.

**Table 2.** Classification by size.

Category	Size	Specifications
Very small (Micro or Nano) UAV	<50 cm	flapping or rotating wings, very low weight
Small (Mini) UAV	50 cm–2 m	fixed-wing model, launched manually by throwing them into the air
Medium UAV	5 m–10 m	load capacity 100–200 kg
Large UAV	10 m<	intended for military operations

### 3.2. Based on Range and Flight Time

The literature [21] divides the classification according to the range and maximal flight time, as shown in Table 3. Regarding this classification, pilots need to take care of the goals and missions that they can achieve. Therefore, these factors are important input parameters for selecting UAVs.

**Table 3.** Classification by range and flight time.

Category	Range (km)	Flight Time (h)
Very close-range UAVs	5	0.3–0.75
Close range UAVs	50	1–6
Short range UAVs	150	8–12
Mid-range UAVs	650	24
Endurance UAVs	300	36

### 3.3. Based on Weight

One of the primary classifications of civil UAVs based on the classification of aircraft can be considered the classification compiled according to the work of Eisenbeiss [22] from 2009, which is shown in Table 4. Weight is often a determining parameter when it comes to aviation agency regulations. Currently, we can consider the most widespread category of UAVs, so-called micro or mini UAVs. These types of small UAVs have several advantages in comparison with large UAVs. They are more suitable for transport. One or two people can handle their transfer over shorter distances by ordinary passenger car. The

most significant advantage of small and light UAV technology is the possibility of choosing the time of the flight and its repetition. Micro- and mini-UAVs are preferable choices for mapping purposes.

**Table 4.** Classification by weight.

Category	Weight (kg)	Range (km)	Flight Altitude (m)	Flight Time (h)
Micro	<5	<10	250	1
Mini	5–25	<10	500	<2
Close-range	25–150	10–30	3000	2–4
Short-range	50–250	30–70	3000	3–6
Medium-range	150–500	70–200	5000	6–10

3.4. Based on Wings and Rotors

UAV platforms can be divided into four categories according to wings and rotors, as stated by [23,24]. Each platform differs not only in the number of rotors but also in its location on the device. Figure 1 and Table 5 show the types of UAVs based on the number of wings and rotors, their advantages and disadvantages, and their cost.

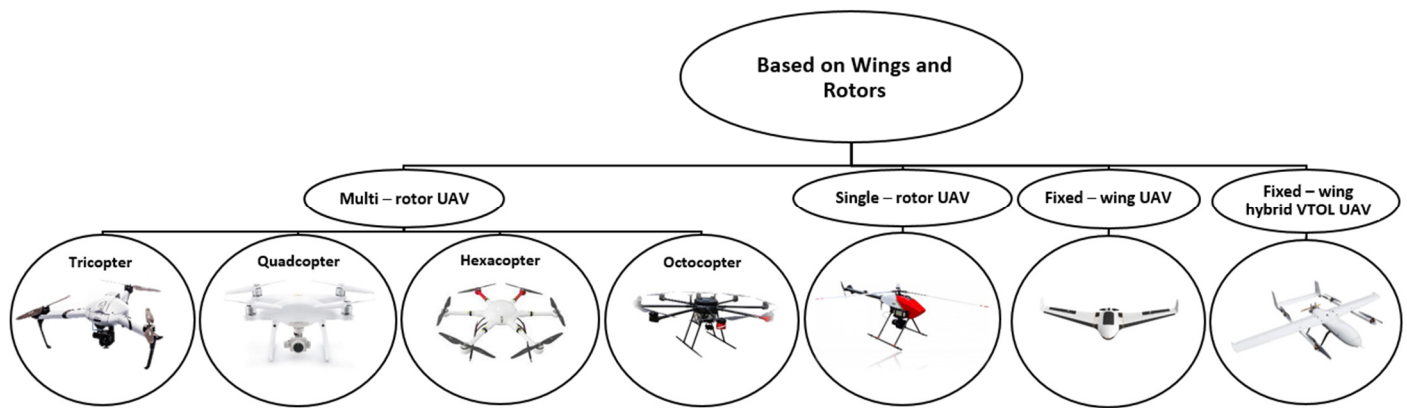


**Figure 1.** Classification based on Wings and Rotors.

**Table 5.** Classification by wings and rotors [23,24].

Category	Rotors/Wings	Advantage	Disadvantage	Price
Multi-rotor UAV	2–8	availability, ease of use, good camera control	lower efficiency in terms of energy consumption	5000–65,000 EUR
Single-rotor UAV	1	ability to fly with heavy payloads	requiring a lot of maintenance and care, operated with a pilot’s license	25,000–300,000 EUR
Fixed-wing UAV	1	covering greater distances, mapping larger areas, higher speed, longer flight time, energy efficient	need of runway or catapult to launch the UAV, price, necessary training to fly	25,000–120,000 EUR
Fixed-wing hybrid VTOL UAV	2<	built-in autopilot function, longer flight times	only a few hybrid VTOL UAVs on the market, not perfect for either forward flight or hovering	25,000 EUR<

#### 3.4.1. Multi-Rotor UAV

Multi-rotor UAVs are the simplest and cheapest UAV option. Multi-rotor UAVs are especially useful in flight as they offer more control over the UAV's position and are ideal for aerial photography and surveillance. Since they have more than one engine, they are called multi-rotors. Classification divides them into quadcopters (four rotors), hexacopters (six rotors), octocopters (eight rotors), and others. Quadcopters are by far the most popular multi-rotor UAVs. The advantage of multi-rotor UAVs is their availability, ease of use, reasonable camera control, support for vertical take-off and landing (VTOL), and the ability to work even in limited space. Compared to other UAVs, the disadvantage of multi-rotor UAVs is their lower energy consumption efficiency so that they can fly for only about 30 min with a small payload capacity. The procurement price of multi-rotor UAVs varies between EUR 5000 and EUR 65,000. These UAVs can be used to monitor bridges, power lines, wind turbines, offshore rigs, and more, as well as 3D scanning and photogrammetric measurement of urban areas and small structures [23,24].

#### 3.4.2. Single-Rotor UAV

Single-rotor UAVs are solid and durable. Single-rotor UAVs resemble helicopters in terms of design and structure. Therefore, the launch of a single-rotor UAV is similar to that of a helicopter and requires special training. Single-rotor UAVs have just one rotor, which is like one large-diameter rotating wing or propeller, plus a tail rotor to control direction and stability. The aerodynamics of single-rotor UAVs allows the use of very long blades that resemble a rotating wing rather than a propeller, making single-rotor UAVs highly efficient. Single-rotor UAVs have an advantage over multi-rotor UAVs if the UAV is gas-powered, which guarantees a longer flight time and higher flight speed. Another advantage of single-rotor UAVs is the ability to fly with heavy payloads (e.g., an airborne lidar laser scanner). A single rotor is more efficient at lifting a heavy load and consumes less battery or fuel during flight. These single-rotor UAVs can also pose safety risks and must be operated only by a licensed pilot. The disadvantage of single-rotor UAVs is that they are mechanically complex, requiring much maintenance and care. Another disadvantage is their price, which ranges from EUR 25,000 to EUR 300,000. Single-rotor UAVs are mainly used by surveyors and civil engineers who want to lift heavier payloads of up to 40 kg into the air. However, today's most advanced technology in fixed-wing and multi-rotor UAVs gives surveyors more flexibility at the survey site [23,24].

#### 3.4.3. Fixed-Wing UAVs

Fixed-wing UAVs have a single fixed wing that resembles that of a piloted airplane in design and function. Fixed-wing UAVs cannot hover in the air—they can only move forward with the achievement of lift and energy efficiency. However, this makes it difficult to launch these UAVs. Depending on the size of the UAV, it is necessary to launch the UAV using a runway or catapult. The advantages of fixed-wing UAVs include covering greater distances, mapping much larger areas, reaching a higher speed, and having a longer flight time. This type of UAV can fly at higher altitudes than other UAVs (often limited by flight restrictions). However, fixed-wing UAVs can be expensive (EUR 25,000–120,000). Another disadvantage is that training is usually required to fly a fixed-wing UAV. Fixed-wing UAVs are ideal for long-range precision aerial mapping and photogrammetry. With a flight time of 90 min, they can cover a large part of the Earth, have a range of 7.5 km, and can map the topography of the Earth's surface with an accuracy of  $\pm 2\text{--}5$  cm. They are used in aerial mapping, forestry and environmental surveys, monitoring pipelines, and power lines in agriculture or construction [23,24].

#### 3.4.4. Fixed-Wing Hybrid VTOL UAVs

Hybrid types of VTOL UAVs combine the advantages of fixed-wing and rotor designs. This type of UAV uses small rotors that are attached to fixed wings. It allows the UAV to hover, take off, and land vertically. After takeoff, VTOL UAVs continue to glide like

typical aircraft using aerodynamics, making them very efficient. There are few of this new category of hybrids on the market, but as technology advances, this option may become much more popular. The advantage of this technology is that it has a built-in autopilot function that maintains the UAV's stability, while the human pilot's task is only to control the UAV during flight. Hybrid VTOL UAVs are perfect for either hovering or forward flight. There are only a few hybrid VTOL UAVs on the market, and the technology is still developing. It is expected that this type of UAV will be able to serve as the delivery vehicle for shipments [23,24].

#### 4. Regulations of UAV Flights

UAV technology has been developing since its inception, along with the legislation determining conditions for flying with these devices. The beginnings of flying with UAVs were rooted in using this technology for recreational purposes when the equipment was affordable and the requirements for the flight were not clearly defined. The flight could be made by anyone who owned a UAV. By gradually applying UAVs in various areas such as land management, engineering geodesy, photogrammetry, and others, legislative regulations for flying in the airspace with this type of equipment have been determined [25,26]. Legislation differs between the amateur use and the professional or commercial use of UAVs. Many countries have been forced to introduce specific laws and regulations to regulate the use of UAVs for different types of users. Established rules must be updated with each advancement in UAV technology. Some countries have created institutions that issue certificates for pilots, register UAV devices, and control the use of UAVs in their airspace [27,28]. The Global Drone Regulations Database was created for this purpose, which records an overview of the legislation, authorized institutions, and necessary information about the selected country. This review also mentions UAV regulations in Europe and the Slovak republic, mentioning specific requirements for neighboring countries.

##### 4.1. European Union

Carrying out a flight with a UAV in the airspace above the territory of the European Union is subject to compliance with the regulations issued and administered by the European Aviation Safety Agency (EASA). To fly in this space, the UAV operator must meet the set conditions in the registration of the pilot and the UAV if it weighs more than 250 g or the device is equipped with a sensor (camera) to capture personal data. Each member state, based on Regulation no. 947, issued by the European Union Commission in 2019, is to compile a register of operators and a register of certified UAVs with their respective identification [29]. To obtain a certificate and permission to fly in the airspace of each country of the European Union, the UAV operator must undergo training provided by the relevant institution in the member country. The regulation also orders that each UAV should contain a member state code and the pilot's unique 12-digit digital registration number. The UAV should be in the pilot's field of vision, called the Visual Line of Sight (VLOS); the flight height should not exceed 120 m from the nearest point on the Earth's surface; and the flight should not occur near other objects. It is forbidden to fly over airports, groups of people, and residential or military zones without permission since privacy or security is violated when pictures or videos are taken. According to Regulation 2019/947, UAVs can be divided into three operational categories (open, specific, and certified) based on flight risk. This risk is determined by the weight of the UAV and the location of the flight. Depending on the flight category, a remote pilot may need specific permits or certificates [30,31]. The review contains selected European Union member states such as Slovak, Czech Republic, Poland, Hungary, Austria, and Germany.

##### 4.1.1. Slovak Republic

The Slovak Republic is one of the member states of the European Union that has adopted and implemented laws and regulations on flying UAVs in its airspace. The conditions for UAV flying are determined by Decision no. 2/2019 [32] of the Transport

Authority (NSAT) in Bratislava, which also prohibits specific aircraft categories from flying in protected zones. These zones are shown in the online air map maintained by the Aviation Information Service of the Slovak Republic [33]. Carrying out a UAV flight in the airspace is also provided for in the Aviation Act no. 143/1998 Coll [34]. If the pilot, in addition to photos and videos, plans to use the UAV to create accurate maps, orthophoto maps, digital models of the Earth's surface, 3D models, they still need a security clearance from the national security office with a contract with the Ministry of Defense on access to classified information.

#### 4.1.2. Czech Republic

To fly in the airspace with a UAV over the territory of the Czech Republic, obtaining a permit from the Civil Aviation Authority (ÚCL) is necessary [35]. As a rule, it is a mandatory registration for the user who will fly with the device for recreational or commercial purposes. In the case of commercial flying, the obligation to possess a permit to operate aerial work or for one's activity is also waived. All these actions are online in regulation no. 947 of the Commission of the European Union [29]. Registration is not required if the UAV weighs less than 250 g and does not have a camera or other device to capture personal data. Each registered pilot receives a registration number to be placed on all UAVs owned by the pilot [36]. For each pilot, the Dronetag company has released the Dronald application [37], which serves to provide information about the valid pre-operation rules for a specific type of UAV in the Czech Republic. Restrictions include flying up to a height of 120 m, an up-to-date overview of the situation with visibility on the UAV, observing safety rules, flying near airports, and others [38]. An online map [39] of the territory of the Czech Republic was created for pre-flight preparation, which shows zones with restricted or prohibited flying. These restrictions are also established in Act no. 49/1997 Coll., on civil aviation [40].

#### 4.1.3. Poland

All regulations, prohibitions, permits, and restrictions in Poland are managed by the Civil Aviation Authority (CAA) [41], which coordinates all actions performed with UAVs. Poland has also adopted the UAV regulation issued by the European Aviation Safety Agency (EA-SA). In addition to these mentioned regulations, the country also has specific rules, one of which is to perform UAV operations at least in 5 km distance from airports, UAV operations at a distance of 100 m from populated areas and 30 m from animals, vehicles and people. In addition, liability insurance is required for commercial operations, and a commercial pilot must obtain a medical certificate and a theoretical and practical test certificate [42]. Each UAV operator is obliged to inform the Polish Air Navigation Services Agency (PANSNA) before the flight [43,44].

#### 4.1.4. Hungary

The airspace over the entire territory of Hungary is managed by the Hungarian General Directorate for Air Transport (GDAT) [45]. According to Hungarian regulations, it is forbidden to fly UAVs up to a height of 50 m or more above the ground or water level in the Open category. In the Specific category, this level is 120 m and more if The Department of Civil Aviation has not granted an exception. According to the EASA regulation, a UAV in the Open category can be flown up to a height of 120 m. Hungarian rules order that the UAV should not be more than 500 m away from the pilot during operation [46]. The validity of the UAV operator's registration number is only one year, after which it must be renewed [47]. An online map [48] of the airspace over the territory of Hungary was created to provide an overview of the availability and location of airports, restrictions, and drone-free zones.

#### 4.1.5. Austria

Before actually flying with a UAV in Austria, it is necessary to register and obtain a permit from the Austrian Civil Aviation Society (Austro Control) [49,50]. For the operator,

registration is valid for 3 years. An operating license is not required in the Open category if all limits such as weight and flight height are respected. There may be areas throughout the country where a special permit is required [51,52]. For the safety of air traffic, the Dronespace application and online map [53] were created, which display current map data, the structure of the airspace, and the position of other UAVs using the Fly-Now function.

#### 4.1.6. Germany

In Germany, flying UAVs is legal under certain conditions mandated by the Federal Aviation Administration (LBA) [54]. Among them is the obligation to ensure every UAV performs an airspace operation. It is the duty of the operator to mark the owned UAV with a fireproof badge with the operator's name and address [55]. Prohibited and restricted zones for flying in Germany are shown on online maps [56,57].

### 5. Selected UAV Sensors and Their Applications

Nowadays, there are a large number of UAVs that are specific in terms of their shape, mass, size, height, or range. Tables 6 and 7 show different types of UAV carriers according to specific parameters during measurement, under different conditions, and in different parts of the world with high-quality results. Data obtained from the selected papers are graphically presented in Figure 2. The result is a graphic representation of the main parameters obtained using the selected sensors.

**Table 6.** Specific parameters of measurement with UAV equipped with a camera.

UAV	Camera	Flight Height (m)	GSD (m)	RMSE (m)	References
DJI Phantom 4 Pro	1" CMOS	35	0.010	0.011	[58]
DJI Phantom 4 Pro	Parrot Sequoia	50	0.040	0.370	[59]
3DR Solo	Parrot Sequoia	50	0.065	0.250	[60]
DJI Phantom 4 RTK	1" CMOS	45	0.018	0.080	[61]
DJI Inspire 2	Zenmuse X5S RGB	120	0.023	0.020	[62]
Droidworx Skyjib Oktokopter	Canon 550D	30	0.010	0.140	[63]

**Table 7.** Specific parameters of measurement with UAV equipped with lidar.

UAV	Lidar	Flight Height (m)	GSD (m)	RMSE (m)	References
GV1300	Velodyne Puck VLP-16	80	0.141	0.012	[64]
Droidworx Skyjib Oktokopter	Ibeo LUX	30	0.076	0.420	[63]
RIEGL RiCOPTER	VUX-1UAV	55	0.024	0.750	[65]
OktoKopter Droidworx/MikroKopter AD-8	Ibeo LUX	50	0.141	0.340	[66]
Baloon	Velodyne HDL-32E	25	0.032	0.015	[67]

The graph shows the comparison of GSD, RMSE, and flight height for chosen sensors. The best results according to GSD were obtained when measured with the DJI Phantom 4 [58], DJI Phantom 4 PRO [61], and Droidworx Skyjib Oktokopter [63], where the GSD achieves an accuracy of less than 2 cm. On the other hand, according to RMSE, the best accuracy is achieved in measurements with the DJI Phantom 4 [58], DJI Inspire 2 [62], GV1300 [64], and Baloon [67], where the RMSE accuracy does not exceed 2 cm.

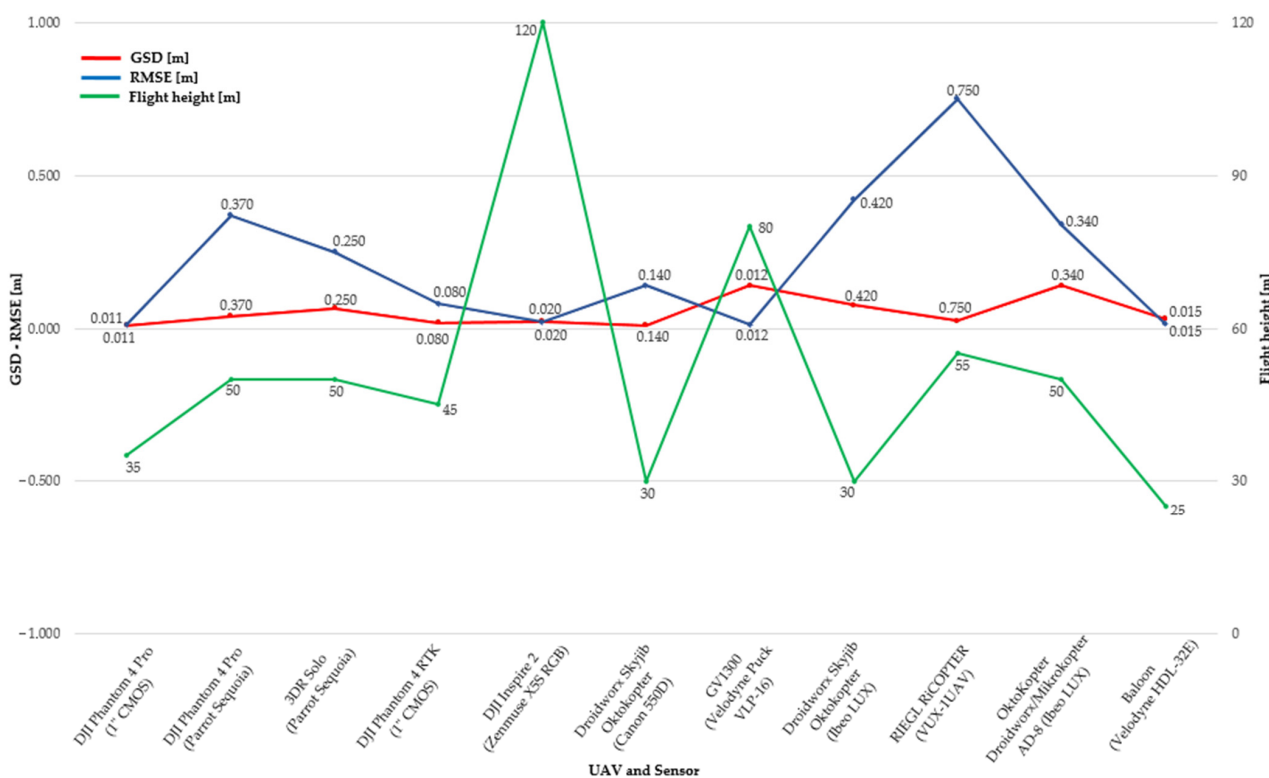


Figure 2. Comparison of sensors GSD/RMSE vs. flight height.

Ground Sampling Distance is the size of the image pixel projected in object space. The larger the GSD size, the smaller the spatial resolution of the image. UAVs have GSDs ranging from 1 to 5 cm. GSD affects, but does not define, the accuracy of the measurement. Horizontal accuracy can often be less than the GSD, but vertical accuracy is usually significantly worse. However, acquired high-quality image grids that are well supported by GCP points can achieve vertical errors less than the GSD. The size of the GSD is related to the choice of camera (e.g., focal length and pixel spacing) and flight altitude [16].

Root Mean Square Error is required as a global quality indicator that indicates the accuracy value. It is generally reported that the smaller the RMSE value, the more accurate the measurement. It is the distance between the input position of the GCP ground control point and the retransformed position for the same GCP. It states how closely the retransformed location matches the desired output point location [16].

In [58], the authors investigated and monitored the development of erosion, morphological changes in talus cones, and the dynamics of the movement of rock blocks and talus cones between individual stages of measurement in the Small Cold Valley in the High Tatras in the north of Slovakia at an altitude of 1600 m (AMSL). The total area of investigation was 5000 m<sup>2</sup>. Geodetic and photogrammetric methods were used to document the current state of the site and generate DEM. The survey aimed to capture the morphology of the terrain in high level of detail. A DJI Phantom 4 Pro UAV equipped with a digital camera with a resolution of 5472 × 3648 pixels was used to capture 1389 images from a height of 35 m. The parameter of ground sampling distance (GSD) was 0.01 m. The overlap of the images was set to 80%. For georeferencing, 16 GCPs were used. Their coordinates were determined using the spatial polar method, and their average total RMSE was 0.011 m. Data processing was carried out in the Agisoft Metashape Professional 1.5 software. The resulting point cloud contained 261 million points.

The study [59] used a DJI Phantom 4 Pro equipped with a compact Parrot Sequoia multispectral sensor, which can capture RGB images with a resolution of 4608 × 3456 pixels, to capture rice and wheat yields. The DJI Phantom 4 Pro together with the Parrot Sequoia

sensor weighed 1.746 kg. The authors performed flights at the altitudes of 30 m, 50 m, and 100 m. We focused on their flight at an altitude of 50 m AGL. Multispectral sensing of the area was performed in 10 min. Approximately 3 ha was covered, with the front overlap at 86% and the side overlap at 76%. On average, the root means square error (RMSE) at the control points was 37.2 cm. The ground sampling distance (GSD) was 4.3 cm in this case.

The Parrot Sequoia multispectral sensor was also used by the UAV 3DR Solo quadcopter, which is described in the literature [60]. The study was conducted in a private lychee orchard located 25 km southeast of Brisbane, consisting of 189 trees. The development and dynamics of tree growth and structure were monitored using UAV technology. At a height of 50 m AGL and a flight speed of 5 m/s, 278 images were acquired with 80% side and 85% forward overlap. The created DTM had a GSD of 6.5 cm, and the RMSE value was 0.25 m.

The authors of [61] describe the application of surveying methods to study rock decay and geological hazards due to the erosive force of the Candigliano River in a natural slope in Italy. They used terrestrial laser scanning (TLS) and UAV-based digital photogrammetry. The flights were performed by the UAV DJI Phantom 4 PRO equipped with a 20-megapixel digital camera. Four flights were carried out at flight heights from 10 m to 80 m. A total of 1232 photographs were taken using 80 ground control points (GCPs). A front overlap of 80% and a lateral overlap of at least 60% were set. The average GSD of value 1.8 cm was achieved. Agisoft MetaShape 1.5.3 software was used to process UAV images, where a dense 3D point cloud was generated. The final point cloud contained 22,308,471 points, and the Root Mean Square Error (RMSE) was 80 mm.

The literature [64] shows the use of a UAV on which a scanner was placed. The study area covered approximately 1963 ha and was located in the forests of eastern China. Lidar data were acquired using a Velodyne Puck VLP-16 laser scanner mounted on GV1300 multi-rotor UAV. The flight height was set to 80 m AGL, the flight speed to 4.8 m/s, and the overlap to 75%. Under such conditions, the average point density was 50.24 pts/m<sup>2</sup>. Field data were processed in LiDAR360 software. The obtained result from the flight in this study showed that the data reached similar accuracy, but the use of lidar technology is financially expensive.

Similarly, authors in the literature [62] monitored 178 trees in Furano City, Hokkaido Island, northern Japan. All 3292 images with a resolution of 5280 × 3956 pixels were acquired using the Inspire-2 UAV with a mounted Zenmuse X5S RGB camera at a flight height of 120 m AGL and 80% overlap. The average achieved GSD was 2.3 cm. A total of 19 ground control points were placed in the area of interest. The resulting models were evaluated using the RMSE error. Its value did not exceed 2 cm in both cases. For photogrammetric processing of UAV data obtained by the Zenmuse X5S RGB sensor, the authors used the 3D modeling software Agisoft Metashape Professional Edition 1.5.3. The resulting point cloud had an average point density of 547.01 pts/m<sup>2</sup>.

The study [63] describes the scanning of trees in an area of 1500 m<sup>2</sup> using a multi-rotor UAV Droidworx Skyjib Oktokopter with a Canon 550D digital SLR camera, which captures images with a resolution of 5184 × 3456 pixels. The flight height of 30 m was set at the front at 95% with side overlaps at 66%. In total, 425 images were acquired. Data processing was performed in Agisoft Photoscan Professional v.1.0.0 software with the result of 85 million points with an average density of 5652 pts/m<sup>2</sup>. In the area of interest, 14 ground control points were used. As a result, in block alignment, a horizontal RMSE of 0.40 m and a vertical RMSE of 0.14 m were obtained. The authors also placed an Ibeo LUX laser scanner on the Droidworx Skyjib Oktokopter multi-rotor and scanned the same area of interest from the same flight height. Average density in the point cloud using this device was 174 pts/m<sup>2</sup>. However, the vertical and horizontal RMSE error on 10 GCP points have almost the same value as when using the photogrammetric approach, in which there was a horizontal RMSE value of 0.42 m and a vertical RMSE = 0.17 m.

The tropical savanna forest in the Litchfield Savanna SuperSite, located in the Litchfield National Park in Australia, was investigated using lidar and two UAV flights by the authors in [65]. UAV data were collected using a RIEGL RiCOPTER with a VUX-1 UAV scanner. A

high-resolution flight over an area of 98,000 m<sup>2</sup> at a flight speed of 3 m/s had an average point density of 1800 points/m<sup>2</sup> and was conducted at 55 m AGL. In this case, the RMSE was 0.75 m.

The paper [66] aim was to obtain spatially dense and accurate measurements for forest inventory applications and create point clouds using UAV-borne lidar. The authors used an OktoCopter Droidworx/Microcopter AD-8 multi-rotor VTOL UAV with an Ibeo LUX laser scanner. The Ibeo LUX laser scanner has a maximal range of 200 m and a maximal scanning range of 110°, scans in four parallel layers, and has a beam divergence that reaches 0.8°, a scanning frequency set to 12.5 Hz, and an angular resolution of 0.25°. An area of 100 × 100 m at the University of Tasmania was surveyed during four flights at an average flight height of 50 m with an approximate speed of 3.3 m/s. The resulting point cloud has a point density of approximately 50 points/m<sup>2</sup>. The horizontal RMSE on all 130 GCPs is 0.34 m and the vertical RMSE = 0.15 m.

## 6. Discussion

### 6.1. Discussion on Regulations and Restrictions of UAV

A general overview of the legislative prohibitions for flights with UAVs in selected countries is shown in Table 8. Some of the European Union member countries are described, where the individual prohibitions are almost identical due to the adoption of the EU regulation. Because each country also has its own laws, these prohibitions differ in several ways. Some non-European countries are also mentioned. Each of these countries has adopted its own regulations by which it is governed. Finally, Table 8 also shows the institutions of these countries that manage, control, and issue regulations and certificates.

### 6.2. Discussion on Applications of UAVs

UAV technologies are the most powerful and effective tools for the fast, accurate, and safe capture of aerial data. They can create high-resolution aerial maps, real-time virtual tours or 3D models with an accuracy of centimeters. This area is the most widespread in the use of UAVs and has been addressed by many authors. Areas of use that we dealt with in this review are shown in Figure 3.

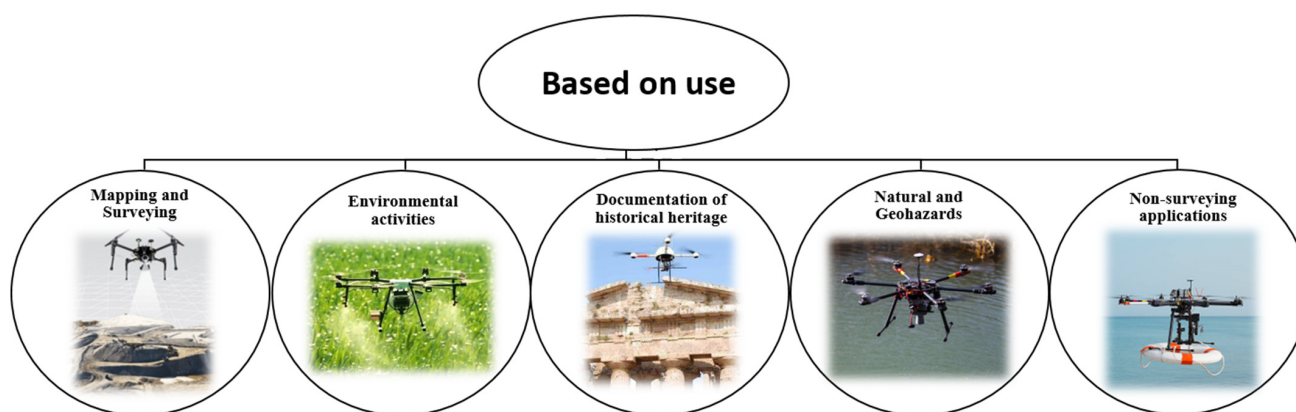


Figure 3. UAV categories based on use.

**Table 8.** Regulations in individual countries.

Country	Institution	Prohibition (without Permission)	References
Slovak Republic	NSAT	<ul style="list-style-type: none"> <li>- flying with UAV if a pilot is under the influence of psychoactive substances</li> <li>- flying at an altitude of 120 m or more</li> <li>- flying with UAV that has a pulse or rocket engine</li> <li>- flying at night</li> <li>- flying without visibility of the UAV with the naked eye</li> <li>- flying for the purpose of commercial air transport</li> <li>- flying for the purpose of spraying chemicals or dropping objects</li> </ul>	[31–33]
Czech Republic	CAA	<ul style="list-style-type: none"> <li>- flying in densely populated areas</li> <li>- flying at an altitude of 120 m or more</li> <li>- flying for the purpose of transporting persons</li> <li>- flying for the purpose of dropping objects</li> <li>- flying over gatherings of people and emergency interventions</li> <li>- flying within 30 m of persons</li> <li>- flying near controlled and uncontrolled airports</li> </ul>	[35,36,38,40]
Poland	PANSA	<ul style="list-style-type: none"> <li>- flying at an altitude of 120 m or more</li> <li>- flying without visibility of the UAV with the naked eye</li> <li>- flying with UAV heavier than 25 kg</li> <li>- flying around airports within 5 km</li> <li>- flying 100 m or less from populated areas and 30 m or less from people, vehicles, and animals</li> </ul>	[41–43]
Hungary	GDAT	<ul style="list-style-type: none"> <li>- flying at an altitude of 120 m or more</li> <li>- flying at night,</li> <li>- flying at a distance of 500 m or less from buildings, people, animals, and structures</li> <li>- endangering people’s lives by flying</li> <li>- flying around airports within 8 km</li> <li>- flying around heliports within 3 km</li> <li>- flying over groups of people, industrial sites, private properties, and government buildings without permission</li> </ul>	[45–47]
Austria	Austro Control	<ul style="list-style-type: none"> <li>- flying without line-of-sight on UAV (VLOS)</li> <li>- flying at an altitude of 120 m or more</li> <li>- flying over groups of people</li> <li>- flying for the purpose of transporting dangerous goods</li> </ul>	[49,50]
Germany	LBA	<ul style="list-style-type: none"> <li>- flying at an altitude of 120 m or more</li> <li>- flying without line-of-sight on UAV (VLOS)</li> <li>- flying for the purpose of transporting dangerous goods</li> <li>- flying in controlled airspace at an altitude of 50 m or more</li> <li>- flying at night with UAV heavier than 5 kg</li> <li>- flying without insurance</li> <li>- flying around airports within 1.5 km</li> <li>- flying with UAV that records or transmits optical, acoustic, or radio signals</li> <li>- flying at a distance of 100 m or less over motorways, waterways, and railways</li> <li>- flying over disaster areas, prisons, residential areas, and more</li> </ul>	[53,55]

### 6.2.1. Mapping and Surveying

The authors of [67] tested a lidar system that was placed on a helium balloon on Sherman Island near Antioch, California. They used a Velodyne HDL-32E lidar scanner with a pulse frequency of 700 kHz and a range of up to 100 m at a flight height of approximately 25 m AGL. The RMSE had a value of 0.09 m. The nominal density of points was 1000 points/m<sup>2</sup>. In their publication [68], the authors investigated the detection of the globalized probability of boundary (gPb) contours using a UAV. They mapped three rural areas in Germany, France, and Indonesia. In Toulouse, France, data were captured with direct georeferencing using a DT 18 PPK and a DT-3Bands RGB camera, with a resulting GSD error of 3.61 cm. In Amtsvenn, Germany, a GerMAP G180 UAV model with a Ricoh GR camera was used with a resulting GSD error of 4.86 cm. Data in Germany and in Indonesia were captured using GCP. For mapping in Lunyuk, Indonesia, they used a DJI Phantom

3 UAV with a Sony EXMOR FC300S camera. The resulting GSD was 3.00 cm. The measurements resulted in three ortho-images of different scales. The authors of [69] demonstrated improvements to the UAV multispectral mapping technique for higher resolution imagery in the terrain over the Indian River Lagoon along the central Atlantic coast of Florida. They use a Parrot Bluegrass quadcopter with a Parrot Sequoia+ multispectral sensor and a DJI Phantom 4 Pro quadcopter equipped with an RGB CMOS camera sensor. As a result, data were collected from a flight altitude of 120 m from which ortho-mosaics, Digital Surface Model (DSM), Digital Elevation Model (DEM), and point clouds were produced. In the study [70], waterfowl in the west of the Songnen Plain, Jilin Province, China, was monitored using UAV technology. A Phantom 4 Advanced UAV equipped with an FC6310 camera and a Nikon MONARCH 82ED-A monocular telescope were used for this survey. Tucci et al. [71] used the UAV to monitor and calculate the stockpile volumes of material from sorted waste collection, producing 3D models from point clouds. They used a DJI Phantom 4 Pro UAV. Zanutta et al. [72] monitored coastal and beach changes using a DJI Matrix 600 and a Spark UAV to produce DTM and ortho-images, and the authors [73] used the DJI Phantom 2 UAV to map flood risks. The use of UAV photogrammetry or lidar technology in the field of mapping and surveying depends on various factors. When choosing a suitable method, it is important to consider instrumentation, required accuracy, finances, point density, or the interpretation of the resulting outputs. However, the use of photogrammetric methods is more advantageous than the use of lidar technology due to the ease of data acquisition, its flexible and fast use, its low purchase price, and the high density of point clouds.

The deployment of TLS and the SfM photogrammetric method has also been successful in the documentation of underground cave spaces [6,74,75] to create 3D models of them. The authors of [6] used the SfM photogrammetric method to take images with a Pentax K-5 DSLR digital camera with a Pentax SMC DA lens in Ochtiná Aragonite Cave, Slovakia. The authors of [74] conducted a tectonic and morphological investigation of the Luo Shui Kong Cave. They used Agisoft PhotoScan<sup>®</sup> Professional Edition, version 1.2 software to process the images and point cloud, from which a 3D model was made. The UAV is also used in the mapping of surface karst areas. The authors of [76] investigated the area in the southwestern part of the geomorphological unit of the Slovak Karst using aerial and ground-based laser scanning. The airborne laser scanning data were obtained using a Leica ALS70-CM scanner. In total, 1.99 billion points with a point density of 29 points/m<sup>2</sup> were captured in the 68 km<sup>2</sup> area of interest. In reference [77], the authors evaluated and classified the vegetation of karst wetlands in Huixian Karst National Wetland Park, Guilin, South China, using a DJI Phantom 4 Pro UAV and an FC6310S camera. They collected data during 12 flights, which were processed using Pix4D Mapper software to generate orthophotomosaics and DSM. The publication [78] investigated the extraction of vegetation information in a karst area using a DJI Phantom 3SE. They captured images with 4000 × 3000 pixel resolution at a flight height of 150 m AGL. Yang et al. [79] addressed biodiversity maintenance in karst areas. They chose the Maotiao Basin and Nanming Basin in the core of the South China Karst as their area of interest. Using DJI Phantom 4 Pro, they acquired 3507 images. Processing was performed using Pix4Dmapper software to generate digital orthophotomaps with a spatial resolution ranging from 1.5 cm to 5.3 cm. The UAV imagery was used for tree and shrub identification and habitat classification. When documenting underground cave spaces and mapping surface karst areas, we recommend the SfM photogrammetric method. With its help, we can observe wetland vegetation, complex reliefs, and numerous karst caves in karst areas, as well as the extraction of vegetation with higher accuracy and better effect. The advantage of combining UAV and SfM is obtaining information about vegetation in complex terrain areas, saving research time, and obtaining more targeted plants.

UAVs have also been applied in the mining industry [80–83]. The review article [80] compiled 65 articles from 2010 to 2020. The articles used UAV AeroVironment RQ-11A Raven, Honeywell RQ-16A T-Hawk, Sensefly eBee, Skywalker X5, AscTec Falcon 8, DJI Phantom III, Aibotix Aibot X6v2, Albatros VT3, and Tholog THO-R-PX8/10. As sensors,

digital cameras, spectral imaging cameras, lidar, thermal infrared cameras, and gas sensors were mounted. Thanks to UAVs, the air was checked against hazardous substances from explosions in mines and quarries, mapped mineral extraction, or the exploration of the mined-out territory. The authors in the article [81] used a DJI S1000 UAV with camera Sony ILCE A7R to map the Piekary and Jaworzno area in 2016. In 2020, it was a BIRDIE UAV with a Sony DSC-RX1RM2 camera. The deformations of the area caused by mining activity were surveyed. The results of spatial changes ranged from  $-0.5$  m to  $+0.4$  m. The article [82] dealt with the study and protection of sites affected by mining activities in northwestern Spain's Roman gold mining infrastructure. Non-contact technologies are used in such areas due to inaccessibility and remoteness. For the mapping, a DJI Phantom 4 with 12.4 Mpx FC330 camera was used. The flight was controlled using Pix4D field software. Based on the acquired data, seven models were created for the monitored site. All models were created from images from 270 to 536, except model nr. 7, which was generated using 63 images. Therefore, the GSD value of 13 cm is also less accurate for this model. For the others, the GSD ranged from 1.8 cm to 4.9 cm. The flight was performed at a height of 50 m AGL. The number of GCPs range from 4 to 9, and the RMSE was calculated. The worst GCP—RMSE was for model No. 7, whose value ranged from 8.8 cm to 41 cm. The best GCP—RMS was in model No. 5, which varied from 0.6 cm to 11 cm. Most of the models consisted of 3D texture, ortho-mosaic, and DEM.

The UAV has been used to explore open pit mines in the articles [84–86]. The authors of the article [84] focused on the exploration of and research on iron mines in the Beijing area. Surface mining was observed in order to monitor changes and other processes in the area, such as pollution or erosion. The mapping of each open pit mine was carried out using the UAV SfM method. Furthermore, the purpose of this measurement was to mitigate the effects of anthropogenic changes caused by mining based on the geomorphological characteristics of the mines. The article [85] was devoted to a review of the UAVs used in the basin areas with their sensors in 2015–2018. The research used 40 articles published in Australia, China, Finland, and other countries. UAVs have been applied in various sectors such as 3D reconstruction and pollution monitoring. Different types of UAVs such as fixed-wing and multi-rotor devices were compared. Sensors such as digital cameras, thermal infrared cameras, and others were also reviewed. The article is also addressed the future development of UAVs, where improvements could be made in the form of data-processing speed, technical advancement, and others. The article [86] explored the application of a fast, inexpensive, and accurate method to monitor environmental changes affected by mining activities. A site in northeast Beijing was selected, where a UAV captured the area with two series of high-resolution images between 2014 and 2016. Using the SfM method, a DEM was created, from which geomorphic changes were assessed using DoD and SLLAC analyses. When monitoring soil surface deformations in areas affected by underground or surface mining, the application of UAV spatial data collection sensors has the advantage of performing quick field work and having a high detail of outputs while maintaining needed accuracy parameters. UAVs make it possible to document otherwise inaccessible parts of mines. The generation of high-resolution height models (DEM) from the results obtained using UAV is useful in the evaluation of geomorphic changes related to mining activities.

The authors of the articles [87–93] discussed using UAVs in land registration. The article [87] highlights UAV photogrammetry and laser scanning for cadastral mapping purposes in the Czech Republic in 12 test areas. Many points (fence corners, building corners) surveyed by conventional geodetic methods (RTK-GNSS, total station) and by UAV technology were compared. UAV carriers Hexacopter G6, MAVinci SIRIUS, and Trimble UX5, where sensors such as Canon EOS 700D, LumixGX1, SONY ILCE-6000, and DMC-GX1 were used for mapping. According to the results, an accuracy of 14 cm was achieved in more than 80% of the measurements. When comparing laser scanning and photogrammetry, the accuracy of the points determined from the lidar-based point cloud was found to be approximately 18% higher than that of the point cloud obtained by the photogrammetric point cloud with the 2 cm GSD. The article also compares the

costs of conventional geodetic measurement methods and the new UAV technology. The research addresses the necessary changes in organizational and technological processes for using UAV technology. In the article [88], the authors investigated and validated the applicability of UAVs for updating cadastral records in areas affected by landslides. The mapped area was in Limanowa in Poland, covering an area of 70 hectares, with the flight height varying over each line individually. The UAV used DJI S1000 with a Sony ILCE A7R sensor, a Sony FE 35 mm F2.8 lens, and a Zenmuse Z15-A7 gimbal. In total, 465 images were taken, of which 388 were used for processing. The purpose was to obtain the analysis results in four variations with a different number of control points and methods of measurement. Orthophoto maps and DSM were used to update the cadastral data. The maximum deviation for each control point did not exceed 10 cm. This research concluded that a larger number of control points should be used to create photogrammetric products, ensuring accurate and correct models. The article [89] demonstrates the use of UAV technology in cadastral mapping, where automatically extracted boundaries are obtained from images. The boundaries were extracted using the ENVI feature Extraction (FX) module. The research was carried out in Slovenia in the municipality of Ponova. The area of the subject territory was 25 ha. A total of 12 GCP were used, evenly distributed over the mapped area, and determined by GNSS/RTK. For photogrammetric imaging, DJI Phantom 4 Pro with a 1" CMOS 20 Mpix sensor was used. The UAV flew at a height of 80 m AGL, with a GSD value of 2 cm. The results of the accuracy evaluation showed that almost 80% of the extracted visible boundaries were correct. In the paper [90], the authors discussed UAV technology to assist in verification surveys of land boundaries in digitized cadastral territories. This case study was conducted in Taiwan in the ChengDa district of Taipei City. The flight was conducted at a height of 300 m AGL using an AIRIDER YJ-1000-HC UAV with a PhaseOne iXU150 medium-format camera. As a result, 230 images were acquired, and the GSD accuracy was 3 cm. The research shows the possibility of generating one cadastral map consistent with the actual details of the terrain. This approach can reduce human resource costs and improve the efficiency of future boundary verification surveys. The article [91] discusses the mapping of large cadastral areas using UAVs. A rice field area of 80 ha in Trimulyo municipality, Indonesia, was selected for the research. In total, nine GCPs with a 12 cm RMSE were used. The flight was performed at a height of 250 m AGL, with a GSD value of 7.77 cm. The flying equipment was an RC high wing with a Nikon COOLPIX AW-120 photogrammetric sensor. This article demonstrates the successful use of a UAV-based remote sensing system to produce ortho-mosaics as base maps for cadastre. The research in the paper [92] discusses a technique based on deep fully convoluted networks (FCN) that can automatically learn high-level spatial features from images to extract cadastral boundaries. For this research, the Busogo study area located in Rwanda was selected. In 2018, Charis used a UAV to image the area and obtained photographs that were subsequently analyzed. The article [93] focuses on implementing UAV-based GNSS CORS UDIP to improve cadastral survey and urban development monitoring. The area of interest for this research was the city of Ngresep, which was flown over using a DJI Phantom 3 Professional with a Sony EXMOR sensor. The flight was conducted at a height of 182 m AGL. A total of 1387 images were acquired and subsequently processed. Fifteen GCPs were placed in the field, and coordinates were determined using the static GNSS method. The result is an ortho-mosaic with a GSD value of 7.86 cm, which can be used to delineate parcel boundaries and create a base map. Lidar and photogrammetry based on UAV can be effective methods in their applications in the field of real estate cadastre. These methods achieve reliable accuracy but lack completeness of the performed survey. Furthermore, the use of UAVs appears to be a suitable method when a large proportion of boundaries are visible. UAV technology is used as an alternative to speed up processes in the field of real estate cadastre. The local investigation of ownership relations and measurement of omitted objects is still necessary.

The authors of the articles [94–100] have devoted themselves to research in the industrial sector. The article [94] dealt with using UAVs to calculate the volume of gravel

reserves. This volume was surveyed using a Leica TS06 total station and a DJI Mavic Air UAV. A total of 128 images were acquired at a height of 50 m AGL. After processing, DEM and TIN models were generated. A volume of 2686.3 m<sup>3</sup> was calculated using the UAV, and a volume of 2830.7 m<sup>3</sup> was calculated using the total station. In the article [95], the authors wanted to create a model to generate an optimal flight plan for UAVs. This model would manage safety in the oil and gas industry. The article [96] reviews UAV platforms and sensor systems designed for the oil industry and environmental monitoring. The described UAVs are divided into different categories, such as fixed-wing UAVs and rotary-wing UAVs. The brands and types of UAVs such as Mavinci Sirius, Trimble Gatewing X100, Aibot X6, and Matrice200 are listed. Sensors such as gas detectors, radar, lidar, and thermal infrared (IR) cameras are also listed. The brands of these sensors, Yuneec CGOETUS, Optris PI 450, FLIR Quark 640, ICI Mirage HC, Workswell GIS-320, MosaicMill Rikola, HySpex Mjolnir VS-620, Riegl VUX-1UAV, VelodyneHDL-32 E, LeddartechVu8, and others, are also listed. The authors in the article also mention the UAV application, which they describe uniquely. The research in [97] discusses the design of a two-mode network analysis framework to quantify the spillover effects of UAV technology in various industries using U.S. Patent and Trademark Office patent citation data. In [98], the authors studied the fog-assisted computing problem of UAV in Industry 4.0 smart factories. The simulation results show that the proposed online algorithm can achieve near-optimal task allocation with an optimality difference of no more than 7.5% compared to offline. The authors of [99] discussed research on monitoring CO<sub>2</sub> gas levels in smart factories because CO<sub>2</sub> harms humans. According to the study, the UAV would securely transmit the sensor data to the MEC server to analyze them and make an automatic decision. The result shows of the analysis show the successful monitoring and detection of CO<sub>2</sub> levels in factories. The research in [100] deals with imaging complex sites and areas in sugarcane factories in San Joaquin and the Aguila aqueduct in Spain. A DJI Mavic Pro Platinum with a 13 Mpix sensor was used for the imaging. According to the results, UAV technology is more accurate, time-saving, and suitable than standard methods. UAVs offer great potential for creating mathematical models in the oil and gas industry. Among other things, gaps and open issues were defined for this technology, which are connected to the field of the detection of oil spills at sea and oil spill detection, monitoring of gas pipelines, sensing of gas emissions, remote control of equipment, exploration of deposits and offshore oil spill detection, oil leakage detection, pipeline monitoring, gas emission sensing, remote facility inspection, and petroleum exploration.

The authors have discussed UAV applications in architecture in [101–107]. The article [101] focused on 3D model and texture generation using a ground-based laser scanner and UAV. The object investigated was the Torre Pelosa watchtower, located in the city of Bari, Italy. The TLS RIEGL VZ-400 scanner, with maximal scanspeed of 122,000 points/sec, was applied. An external Nikon D700 camera with 10 Mpix quality was connected to the scanner. The UAV Microgeo's AeroMax600 with a 12 Mpix Canon S100 camera sensor was used. For indirect georeferencing, GCP was used. The image processing method was SfM. The software environment used for data processing was Riscan Pro v.1.6.1 and Agisoft PhotoScan v.1.0.4. The Resulting 3D model and 3D point cloud were generated. The authors of the article [102] explored a concept for weighted data fusion that can enhance the 3D mapping transmitted by a UAV using a camera and a lightweight line laser scanner. The research used a UAV with a Hokuyo UTM-30LX-EW sensor and a GoPro 1080p HD HERO2. The measurements were made at the Karlsruhe Palace in Germany. From the result, an accurate 3D model was created. The images had an estimated standard deviation of 0.44 pix, and the scanner was 12 cm. The research in the article [103] focused on using UAV for the 3D modeling of Tibetan architectural heritage. The area of interest is located in the monastery town of Gyantse (Tibet), and the surveyed building is the Auspicious Multi-Door Stupa. A DJI Phantom 4 with an integrated camera was used for the imaging. A TLS Leica ScanStation C10 laser scanner with a Canon 60D external camera was also used. A total of 55 GCPs were taken at this location and determined by the total station.

After SfM processing, the resulting RMSE had a value of 2.05 cm/1615 pix. For the TLS, the RMSE was 6 mm. A 3D model of the building was generated. The article [104] was devoted to research on applying oblique aerial photogrammetry. A resort hotel located in Mengyuan area, China, was selected for this research. The UAV DJI Mavic 2 Pro was used and controlled using the Pix4D capture application. Data were processed in Autodesk ReCap software to create a 3D model of the hotel. The author of the article [105] discussed architectural heritage documentation using low-cost UAVs with a fisheye lens. The measurement location was The Otag-i Humayun, Turkey. The UAV used was a 3DR Solo UAV with a 12 Mpix GoPro Hero 4 sensor. Only 28 images were captured, at a height of 50 m AGL. When five GCP were also deployed, the result was a RMSE value of 3.1 cm. As a result, the 3D point cloud, DSM, ortho-mosaic, and a 3D solid model were created. The authors of the article [106] discussed research on monitoring and 3D documentation of architectural heritage using UAV. The equipment contained ISTI-CNR UAV with Ximea XiQ high-speed camera, and Canon EOS M (18 Mpix) was used. Agisoft Photoscan, COLMAP, and Autodesk ReCap software were used for 3D reconstruction. Accuracy was achieved within a few tenths of a millimeter. To accurately assess the architectural features of the peach trees at Washington State University's Tukey Horticultural Orchard, both a UAV with an integrated RGB camera and a lidar system were used for reference [107]. Photogrammetric data were acquired using three flights at a flight height of 15 m AGL, with an overlap of 80%. A DJI Phantom 4 Pro UAV with an integrated 20 MPix RGB camera was deployed. The resulting GSD reached an average value of 0.49 cm. Lidar data were acquired using a UAV on which a VLP 16 Velodyne lidar was placed. The Pix4Dmapper software was used to create a 3D point cloud, a digital surface model (DSM), a digital terrain model (DTM), and ortho-mosaics. In architecture, the use of UAV photogrammetry is especially suitable. Compared to classical methods using total stations and lidar methods, they have the advantage of almost complete coverage of the measured object. The realistic phototexture of the resulting model is also a great advantage.

### 6.2.2. Environmental Activities

The agricultural industry uses UAVs to monitor crops. Agricultural terraces in China were mapped by the authors using a DJI Phantom 4 Pro UAV in [108]. For surveying agricultural fields of winter wheat, in [109], they used a DJI Matrice 100 UAV on which an Odroid XU4 lidar sensor was placed. Other authors, in [110], used DJI Matrice 210 UAV with a CMOS sensor in the Emilia-Romagna region in Northern Italy for mapping and monitoring in precise agriculture. The authors of [111] used a UAV hexacopter with a Canon EOS M color camera for soil and crop mapping in a maize field. As a result, they produced a digital surface model (DSM) of the bare soil and crops and a multispectral orthophotograph. UAVs are also used in agriculture to control irrigation and pests using T16 UAV [112]. Some UAVs can perform fertilization and crop spraying [113]. UAVs allow farmers to carry out critical measures related to irrigation, crop disease [114], or unpredictable weather quickly, time-efficiently, and less labor-intensively. Both UAV photogrammetry and lidar methods are suitable for crop monitoring in the agricultural industry. Lidar is more suitable for crop volume estimation, and UAV photogrammetry is recommended for tracking crop development at different stages or maximizing crop productivity, which requires up-to-date, accurate, and georeferenced crop information. UAVs without any sensors are often used in agriculture. For more efficient work in the fields, UAV carriers are used for irrigation, fertilization, or pest control.

In forestry, UAVs are used to map forest structures [63,64] and tree heights, assess tree pruning [60] and forest inventory [66], or perform various other forestry functions [115,116]. The study [64] used a multi-rotor GV1300 with a Velodyne Puck VLP-16 laser scanner to monitor forest structures in Eastern China. The authors of [63] observed the forest structure. They combined a Canon 550D digital SLR camera and an Ibeo LUX laser scanner on a multi-rotor Droidworx Skyjib octocopter. Johansen et al. [60] investigated tree crown feature extraction using a Parrot Sequoia sensor mounted on a 3DR Solo quadcopter.

They assessed pruning effects on 189 trees in a lychee orchard southeast of Brisbane, Australia. In [66], forest inventory applications were investigated using a multi-rotor VTOL UAV OctoCopter Droidworx/Microcopter AD-8 with an Ibeo LUX laser scanner. In [115], the authors conducted a young forestry trial survey within the central North Island of New Zealand using UAV laser scanning and SfM methods. A Lidar USA Snoopy V-series system with an integrated Riegl MiniVUX-1 scanner mounted on a DJI Matrice 600 Pro UAV was used for the UAV aerial scanning. The data reconstructed by the SfM method were captured using a DJI Phantom 4 Pro UAV with an integrated 1-inch 20 MP RGB camera. A DJI Matrice 210 UAV was used for forestry applications, on which four laser scanners—RIEGL VUX-1 UAV, RIEGL miniVUX-1 UAV, HESAI Pandar40, and Velodyne Puck LITE—were mounted [116]. The collected data were used to demonstrate the effectiveness of deriving forest inventory attributes. For forest inventory and sustainable forest management regarding the provision of accurate estimates of forest attributes, UAV photogrammetry and lidar data are equally applicable. However, the difference is visible in the estimates of the vertical structure (the range of tree crown density), when ALS provides more accurate results than photogrammetry. UAV remote sensing is a suitable tool for monitoring changes in tree structure. Different flight heights can be used, but increasing flight height reduces the accuracy of the tree crown perimeter and area. Both UAV-based methods are reliable for the accurate measurement of the position, height, and width of trees.

Applying UAVs to wild plant counts [117–120] and animals [121–123] is a modern application. In [117], research was devoted to detecting the number of plants from UAV images present in a plantation. The main task was to extract the number of plants found in corn and citrus fields from RGB images. Images were taken from the platform carried by the UAV. The results obtained were in the form of 6224 plants per image. The article [118] describes the digital counting of sunflower plants from aerial images acquired by a UAV using low-height flights. According to the results, it is possible to estimate the number of plants in an image with an error of 10%. The research in article [119] discusses counting and sizing plants in UAV images using an R-CNN mask that detects and segments individual plants. There, three potato fields, two lettuce fields in the UK, and one field in Australia were monitored. The flight was conducted at 50 m height with DJI S900 and DJI Inspire UAV with a Panasonic GH4 sensor and a DJI Zenmuse X4S sensor, respectively. The SfM processing method was used. The aim of the research [120] was to count corn plants using images from UAVs flying at a height of 30 m AGL. The images were obtained by RGB sensors Canon PowerShot S100\_5.2, Sequoia\_4.9, and DJI FC6310\_8.8 carried by 3DR SOLO and a DJI Phantom 4. This research was carried out on a plot of land in the Colegio de Postgraduados, Campus Montecillo. The UAV remote sensing application is a recommended method in the field of precision agriculture precisely because of its ability to detect individual plants and plantation rows with high accuracy.

### 6.2.3. Documentation of Historical Heritage

Research on the documentation of historical monuments has been elaborated in the articles [124–130]. In [124], the authors dealt with the measurement and documentation of the Church of the Holy Spirit in Liběchov, Czech Republic. The measurements were performed using a FARO Focus 3D X 330 laser scanner from the ground and supported by aerial photogrammetry. After processing, a derived document (two plan and four view drawings) and a 3D point cloud model of the church were created. In the article [125], the authors discuss the documentation of hard-to-reach places in historical buildings using an UAV. An octo-rotor UAV with Ouster OS0, Intel RealSense D435, Garmin lidar-Lite v3, Fermion URM37, and Sony A6500 sensors were used for data acquisition. The Church of St. Anne and St. Jacob the Great in Stará Voda and St. Maurice Church in Olomouc in the Czech Republic were monitored. The authors of the article [126] obtained 3D reconstructions of cultural heritage using a BNU D8-1 UAV with a Canon EOS 5D Mark II digital camera and a Riegl VZ-4000 ground-based laser scanner. The Liao family temple, located in Gutian

village, China, was documented. Forty-five images of the object under study were taken from a height of 100 m AGL. The article [127] describes research on photogrammetric mapping of Mondújar Castle, located in Spain. The images were taken using a DJI Phantom 4 Pro+ with a 20 Mpix sensor. The result was a 3D model of the castle with an ortho-mosaic. The article [128] deals with monitoring dark spots in large historical buildings using micro-UAVs. The authors of [129] evaluated the quality of 3D models of monuments obtained using UAVs. The Chapel of the Holy Archangels George and Gabriel, located in Sarajevo, was selected for the research. The UAVs used were the DJI Phantom 4 Pro and the DJI Mavic Pro. As a result, a 3D model with a resolution of 14 mm was created. In the article [130], the TLS and UAV technologies were compared. For this study, the site of the historical fortified tower Torre Zozzoli, located in Italy, was selected. Finally, a 3D digital reconstruction of the object was analyzed. The UAV finds its place in the documentation and 3D reconstructions of cultural heritage—historical monuments (churches, castles, historic fortified towers, and other cultural monuments) with large-scale dimensions and complex construction. Emphasis in research is placed on testing the potential accuracy with the subsequent generation of 3D models of historical monuments. The advantage of UAV remote sensing is mainly the coverage of high-lying parts of objects, the high detail, and the accuracy of models.

UAVs are also used for documentation in archaeology [131–137]; the article [131] presents examples, possibilities, and results from aerial photogrammetry. Using UAV, the geometrical parameters of the archaeological sites of Clunia, Puig Rom, Vilanera and Cosa in Italy were determined, and their 3D models were created. The UAVs used for data acquisition during the period 2014–2021 were DJI Phantom 1 and DJI Phantom 2 with GoPro Hero 2 sensor, DJI Phantom 3 Advanced with MAPIR NGB sensor, MAPIR RE, Yuneec Typhoon H with CGO-ET sensor, Parrot Anafi Thermal with FLIR Lepton 3.5 microbolometer sensor, DJI Mavic 2 Pro with Hasselblad 1" sensor, MAPIR NGB, MAPIR RE, and DJI Mini 2. The authors of the article [132] discussed the creation of ortho-mosaics using an MD4-1000 UAV with a Sony NEX-7 RGB sensor to survey a 1.13 ha archaeological area in Torreparedones (Spain). Images were taken at heights ranging from 30 m to 80 m AGL and were processed in Inpho UASMaster. The RMSE with and without the use of GCPs are described in the results. In the conclusion, the ratio between RMSE and GSD of the UAV flights is presented as equal to value 5. The authors of the article [133] acquired archaeological documentation of six areas using a UAV designed by Gatoreye Unmanned Flying Laboratory with a lidar Scout-32 system. The measurements were carried out in Chiapas, Mexico. The article [134] discussed research on using UAVs for monitoring, change detection, and analysis of sites where archaeological excavations have occurred. The work was carried out in 2014, 2017, and 2020 in the ancient theatre of Uzuncaburç. Three-dimensional point cloud, orthophotomosaics, DEM, and 3D models were created from images. The 3D position accuracy calculated for the control point (CP) used in the four phases of the survey ranged from 5.8 mm to 33.5 mm. The research in the article [135] was devoted to lightweight and inexpensive UAV to be used for documenting and creating photorealistic 3D models of archaeological sites. The images were taken using a fixed-wing UAV and a DJI Phantom 4 with 12.4 Mpix and 24.1 Mpix RGB sensors (Sony A5100). The researched area was in Pakistan, where the Pakistan Memorial at Shakarparian Hills in Islamabad was monitored. The data were processed using the SfM method. A total of 336 photographs were taken from a 7 ha area, generating 17,174,268 points after processing. The texture was created with a GSD value of 1.2 cm. The article [136] focused on a topographic survey of an archaeological site using a Foxtech UAVcopter with a lidar Yellowscan Mapper sensor. The site selected for this study is located in the northern Sardinian region of Usini (Italy). As a result, a DTM was obtained and compared with the DEM. The authors of the article [137] discussed modern geomatic techniques for detecting and investigating emerging archaeological structures on the northwestern slope of Etna in Sicily. The survey was carried out using a DJI Phantom 3 Advanced with 12 Mpix camera. The flight was carried out at a height of 30 m AGL, and the flight was controlled using

the Pix4D capture mobile application. Using GCP, a 3D model was georeferenced in QGIS software. The result was an ortho-mosaic and a DSM. The UAV application has its use in the field of cultural and industrial heritage. Archeology is a field in which UAVs are also closely connected and used primarily in the field of the geometrical documentation of archaeological sites (excavations), the creation of high-resolution digital models and 3D models, the monitoring of the crack patterns of historic structures, and 3D reconstruction of scenes.

#### 6.2.4. Natural Hazards and Geohazards

UAV technology is also used to track and monitor geohazards. The authors of [58,138] monitored the evolution of erosion, morphological changes in debris cones, and the dynamics of movement of rock blocks and debris cones between stages of measurement in the high mountain environment in the High Tatras. There, the authors used a UAV DJI Phantom 4 equipped with a digital camera with a resolution of  $5472 \times 3648$  pixels. The author of [139] monitored seismic faults in the 2021 Maduo earthquake in China based on UAV-lidar technology, InSAR, and field investigation. The study [140] mapped landslides after the 2017 earthquake using high-resolution UAV imagery in the Jiuzhaigou area in Zhangzha City, Jiuzhaigou County, in northwestern Sichuan Province, China. A few days after the earthquake, a Huaao X-UAV flight was conducted, and a high-resolution DEM was derived from the acquired data. The authors of [141] focused on assessing and analyzing rock falls along a national highway in Phitsanulok Province, Thailand. The images collected by UAVs were transformed into digital topographic contours, and a typical cross-section was created using a digital elevation model (DEM). Rockfall boulders were also addressed by the authors of [142], who used a DJI Phantom 4 Pro quadcopter in their study. From a flight altitude of 75 m AGL, they acquired 89 images with a GSD of 3.5 cm, which resulted in the creation of a Digital Surface Model (DSM) and a map of geohazards. When monitoring geohazards, the goal is usually to create a DSM or DTM, for which the SfM method is more suitable. Using the SfM method, we can monitor the development of erosion, morphological changes in objects, and the dynamics of rock movement or landslides. However, an alternative is also the use of LiDAR technology, which can be used to monitor seismic faults during an earthquake.

Monitoring of changes in volcano morphology using UAV is involved in the works [143,144]. Gailler et al. [143] investigated magnetic field measurements using UAVs in the central part of Chaîne des Puys and at the Petit Puy de Dôme volcano. Derrien et al. [144] monitored the deformation of the summit of Piton de la Fournaise volcano and used ortho-images to fit structural and deformation maps of the study area. The unstable blocks of Sciarà del Fuoco volcano on the island of Stromboli, Italy, were investigated using a Saturn UAV and a Canon IXUS 240 camera in [145]. In cooperation with UAVs and ground-based laser scanning, the area of the volcano was monitored by the author [146]. In the Nirano Nature Reserve in Emilia Romagna, Italy, the author acquired more than 350 images using a quadcopter and Canon Power Shot S110 camera. Using images, he produced point clouds and georeferenced ortho-images and DEM, which were used to study volcanic mud complexes. In the work [147], the authors mapped the volcano's crater rim and volcanic dome. In 2012, lidar data were acquired using a LiteMapper 5600 system installed on a Cessna 402B aircraft. Data were obtained at a flight height of 820 m AGL, with 40% lateral and 60% forward overlap, at a density of 5 points/m<sup>2</sup>. Two years later, the same area was captured using a fixed-wing UAV with Canon PowerShot S100 camera. As a result, 328 photographs with a resolution of  $3000 \times 4000$  pixels were obtained. The authors used the integration of the UAV and satellite imagery at a volcano in East Java, Indonesia [148]. They used a DJI Mavic Pro UAV with a built-in RGB camera equipped with a 1/2.3" CMOS sensor to generate the DSM and ortho-mosaics. Reference [149] used an RC high-wing UAV equipped with a digital camera for mapping during a volcanic eruption, which produced a DEM that was effectively applied to assess the post-disaster situation. In the field of volcano monitoring, the SfM photogrammetric method led to the representation of high-resolution

3D terrain models and allowed the acquisition of high-resolution digital elevation models or accurate deformation maps of the volcano. Thanks to the flight at low altitudes, magnetic anomalies and changes in the volcanic context were displayed well, and morphological information could also be derived. LiDAR technology is equally effective in this area of monitoring, but the cost of equipment and the risk of damage to expensive devices is significantly greater.

The authors of [150] used GEO 2 UAV equipped with a SONY A6000 camera to monitor landslides. The landslide area was observed from a flight height of 100 m, with 80% longitudinal and 60% lateral overlap, resulting in 291 images. Kyriou et al. [151] monitored, using UAV technology, an active landslide located in western Greece and generated highly detailed ortho-mosaics and digital surface models (DSM) using the SfM photogrammetric method. Their study used a DJI UAV Matrice 600 equipped with an X5 camera that captures photos with a resolution of  $4608 \times 3456$  pixels and a DJI UAV Phantom 4 with a camera set to with an image resolution of  $4000 \times 3000$  pixels. The data were collected from a flight height of 110 m AGL, with 90% longitudinal and 75% lateral overlap. The authors of [152] used an UAV to document a steep landslide triggered by rainfall and flooding on both sides of the Rječina River valley near Rijeka, Croatia. The authors of [153] attempted to perform landslide detection and prediction using a SibGIS UAS hexacopter equipped with two cameras. Peppia et al. [154] used a Quest 300 mini fixed-wing UAV with a Panasonic Lumix DMC-LX5 camera at a flight height of 90 m AGL to create a digital elevation model (DEM) to demonstrate the movement and changes in the landslide. Rossi et al. [155] monitored geohazards and landslides in Tuscany using a multicopter UAV named Saturn, which was developed at the University of Florence. In their publication, Rau et al. [156] used a fixed-wing UAV with a Canon EOS 450D digital camera to map landslides caused by rainfall. A UAV can provide observations with high spatio-temporal resolution and enable operational monitoring of landslides and provide analyses of surface deformation. The SfM method is very often used to monitor and map landslides. This method is suitable for creating ortho-mosaic, DSM and DEM, which are most often generated during landslides. Using this method, it is also possible to detect and predict landslides.

UAVs are also used to check the stability of slopes. The authors of [157] addressed the instability of the Elva valley road in northern Italy. They performed 19 flights in this area using a DJI Phantom 4 with an FC6310 camera. They acquired approximately 1700 images, from which they produced digital surface models (DSM) at three different scales: a large-scale DSM of the entire road, a medium-scale DSM to assess parts of the slope, and a small-scale DSM to assess individual discontinuities. The publication [158] used an AS350 helicopter with a Leica ALS80-HP airborne lidar system and a DJI Phantom 4 RTK UAV with an FC6310 camera (1" CMOS) to monitor slope disturbance in the Jiuzhaigou area. Point clouds using lidar were acquired from a flight height of 1500–3000 m AGL, and 377 high-resolution images were acquired using the DJI UAV Phantom 4 RTK, where a dense point cloud was made. Car et al. [159] monitored a landslide that occurred on the R201 railway line Zápřešič-Čakovec using a DJI Phantom 2 Vison+ and produced a digital terrain model. The article [160] used the UAV to acquire 3D orthographic images of the slopes and used them to assess slope stability and quantitative hazard assessment at sites in Croatia. Junaid et al. in [161] monitored the stability of a rocky slope along a highway in Pengerang, Johor, Malaysia. A survey using UAV technology was carried out with a DJI Phantom 4 PRO + V2.0 from a flight height of 5–30 m with an image overlap of more than 60%. From 246 acquired images, 3D point clouds and an accurate 3D surface model (DSM) were made. The authors of [162] analyzed the stability of a slope with a block rock massif using the lidar Leica ALS80-HP and UAV Phantom 4. The authors of [163] deployed UAV in the mining area. They created a digital elevation model (DEM) for the area in the northwestern part of India, in the city of Chittorgarh. Where it is not possible to obtain direct contact measurements due to terrain or safety restrictions, a UAV equipped with a LiDAR, or a digital camera, is used to check the stability of slopes. Slope stability control

should serve to mitigate economic losses, property damage, environmental degradation, and severe injuries or deaths. Both methods are effective for monitoring slope stability, but the authors more often use UAV photogrammetry. The advantage of photogrammetric methods is their low purchase price and the high density of point clouds.

Geology is another area where UAV technology is frequently used. The authors [164] used photogrammetric data outputs to create a 3D model of the geological structure in the Lehôtka pod Brehmi perlite deposit in the Žiar nad Hronom district using a Phantom 2 Vision+ UAV and 14 Megapixel FC200 camera. From a flight height of 35 m AGL, 58 images were made and georeferenced using 18 GCP. The study [165] used an AustroDrones X18 multicopter equipped with a Sony Alpha 7R camera for engineering geology applications in the Saigesbach basin, Sellrain valley, in the Alps of Austria. In total, 640 images were acquired in two flights. They deploy also Multiplex Mentor fixed-wing UAV with a Sony NEX5 camera that collected 4000 aerial images during four flights. The UAV images were processed in Agisoft Photoscan. The resulting ortho-mosaics reached a GSD of 0.02 m when imaging the valley and 0.08 when imaging the basin. For DSM, the GSD value was 0.05 m when imaging the valley and 0.20 m when imaging the basin. Tziavou et al. [166] carried out structural geological mapping of a sedimentary outcrop in South Ayrshire (Scotland). They used a UX5 HP fixed wing and a TRIMBLE ZX5 hexacopter, which produced the resulting ortho-mosaics of the study area. High-resolution photographs that can be transformed into digital models of the outcrops [167,168] are most suitable for geological purposes. The authors of [168] tracked outcrops within Dinosaur Provincial Park using a senseFly eBee fixed-wing UAV with an 18.2 megapixel Sony WX220 digital camera and created 3D models using Pix4Dmapper software. Tracking dikes and outcrops making point clouds and 3D models using data collected by the UAV were also addressed in [169]. The authors of [170] analyzed the geological hazard in Stara Baška on the island of Krk, Croatia, using a DJI Phantom 4 Professional UAV. In the field of geology, the SfM method is most often used to create a 3D model of a geological structure, for engineering geological applications and geological mapping, but also for the prediction of geological hazards. The SfM method obtains high-resolution photographs, from which 3D digital models or ortho-mosaics are subsequently generated. In the field of geology, the SfM photogrammetric method is currently the most effective and popular.

The use of UAVs has also opened new frontiers of observation in hydrology. The authors of [171,172] have used UAVs to observe stream flows. They engage hydrological modeling through the DEM of stream bathymetry with water level estimation. The authors of [173–175] have mounted miniature lidar systems on UAVs to estimate water level and bathymetry. They achieved a measurement accuracy of several centimeters. In reference [176], the author used a UAV to monitor the flow restoration of the Hostivický Brook in Prague, Czech Republic, using a DJI Inspire 1 Pro platform with a DJI Zenmuse X5 camera, which produces images with a resolution of  $4608 \times 3456$  pixels. The acquired data were used to generate a dense point cloud, a digital surface model (DSM), and an ortho-mosaic. In the publication [177], the authors used a UAV multi-copter carrying a Sony alpha 7R camera to monitor and reconstruct the topography of the Jyoge River in Hiroshima Prefecture, Japan. From a flight height of 100 m, with a forward overlap of 90%, a lateral overlap of 50–60%, and a flight speed of 4 m/s, they acquired a series of aerial images, which they processed in Pix4D Mapper to produce an ortho-mosaic and a DSM of the river channel morphology. In hydrology, UAV photogrammetry is used in the same way as lidar technology is used to estimate the water level or reconstruct the topography of the river. The use of lidar is based on information about signal intensity. From the water surface, the signal reflectivity is very low; therefore, the resulting point cloud models drop out, and it is very easy to detect the boundary between water and land. With UAV photogrammetry in hydrology, complete surface images are captured from the camera, and a DSM or ortho-mosaic is then created. The choice of method depends on the observed territory, finances, or the resulting output.

### 6.2.5. Non-Surveying Applications

The advantage of using UAV technology to make photographs [178–180], video recordings [181,182], or cinematography [183,184] consists in the possibility of exploring and capturing territories and areas with high flexibility and range while producing long continuous shots at a reasonable cost. Imaging ranges are from a few centimeters to more than 100 m. Flener et al. in [178] used a Maxi-Joker 3DD minicopter with a 12.3 megapixel Nikon D5000 camera to create continuous, high-resolution digital terrain models (DTM) of river channels and their floodplains. The authors of [179] used a DJI Phantom 3 Advanced UAV with a SONY EXMOR 1/23" sensor to map tree heights and tree canopies. Zhang et al. [180] created 3D models of buildings based on images acquired by a QingTing-5S quadcopter. The work [182] produced a video preview of a peatland east of Ottawa, ON, Canada, using a Canon PowerShot G11 camera mounted on a Hirobo SDX Radio Control helicopter. For the purpose of taking photos and video recordings, the best option is to use UAV photogrammetry. This method meets all requirements related to the detail and quality of the display of the Earth's surface and various objects and phenomena on it.

UAV technologies are now being used in disaster management, rescue operations, and public safety surveillance. Using UAVs, large-scale operations can also be safely carried out with higher efficiency. Rescue forces can avoid danger and save a lot of time and costs since UAVs offer real-time imagery of critical locations and, by thermal detection, reveal movement even in dense vegetation [185]. The authors used a High One Drone UAV quadcopter with The Flir Vue Pro 336 camera. UAV technology can speed up decision-making and refine the disaster site's localization. The issue of the use of UAVs in rescue operations is also addressed by Sun et al. [186], Zimroz et al. [187], and Lygouras et al. [188]. For search-and-rescue purposes, they used the [186] X-UAV Talon 4, on which a GoPro HERO camera was installed. The GoPro HERO 4 camera was set to video mode with a resolution of  $1920 \times 1080$  pixels. As a result, 2200 photographs were segmented, and an ortho-mosaic model and point cloud were produced. Zimroz et al. [187] discussed the applications of UAVs in search-and-rescue operations in an underground mine. Their study used a DJI Mavic Mini UAV, which was manually controlled and equipped with a microphone to detect humans. In addition, in [188], the authors used a six-rotor Rolfer UAV with a  $1920 \times 1080$  HD GoPro camera to detect humans. For fully autonomous navigation of the UAV and automatic detection of humans in danger, the embedded graphics processing unit platform Nvidia Jetson TX1 was used. The authors of [189] used the Talon and Liu X-UAV platform for search-and-rescue purposes. The authors of [190] addressed emergency recognition in the wilderness using the UAV with a Parrot Sequoia+ multispectral camera in Biatorbágy, Hungary. Cho et al. [191] used UAVs in maritime search-and-rescue operations. In the field of search and rescue, we recommend the use of lidar technology in areas with dense vegetation or in the wilderness. However, in open space, a better method is UAV photogrammetry, which, using a camera or microphone, can detect swimmers in open water and can be effective in emergency search-and-rescue operations.

Currently, UAV technology is also used by military units. The authors of [192] used UAVs for the surveillance of geographic regions and to monitor them for security reasons. UAVs are used for strategic and tactical needs [193–195], simulations [196], surveys [197], and espionage, without the military risking any human lives. UAVs are used in military conflicts to transport and drop bombs and missiles. So-called flying munitions UAVs (also known as kamikaze UAVs), which serve as weapons, are also increasingly frequently used. UAVs are also suitable for land mine clearance when they use hyperspectral imaging technology to quickly identify landmines buried in the ground. With the expansion of UAV technology, their misuse for illegal activities such as jamming, information leakage, or espionage is increasingly occurring. UAVs are also directly used in military operations, where they can be damaged or destroyed; therefore, we recommend using the cheapest possible camera sensor for these purposes.

UAVs are also used to inspect power lines and pipelines [198–203]. The article [198] used a DJI Phantom 4 PRO V2.0 UAV to detect abnormal vibration of dampers on portable

power lines. During flight, a distance of 10 m from power lines and transmission towers was maintained. In the article [199], the authors discussed the application of UAV technology to inspect power lines that were imaged at a low height. A 16.5 km long section was selected for this research in Yichang, China. A fixed-wing UAV with a Nikon D810 digital camera was used to acquire images. In total, 1066 images were acquired, with a GSD accuracy of 3.5 cm. The authors in the article [200] described a new sensor package designed for micro- or mini-UAVs. This package can include a laser scanner, camera, IMU, and other sensors that can vary according to the requirement and application. Hokuyo (30LX) and Sick LD-MRS-400001 on the md4-1000 UAV were also investigated. The authors of [201] dealt with the design of a safe flight approach (SFA) of UAVs in controlling power lines. The authors of the article [202] discussed the development of a platform that provides control of UAVs when inspecting overhead transmission lines. This platform has already been applied in Tianjin, China, where it achieved excellent results. The article [203] proposes a complementary attitude data system based on augmented reality tags (AR Tags) to enhance the reliability of the UAV flight-attitude-determination system, making the results positive. The positional accuracy of the UAV was increased. The results of these studies confirm that UAV lidar technology can locate obstacles in the power line corridor with high accuracy ( $\pm 0.5$  m). The testing of this UAV confirmed its effectiveness in the inspection of electrical lines and the very control of the distribution of electrical lines to ensure the safety of operation.

UAV technology is currently used in everyday life in almost every scientific, technical, and non-technical discipline. UAVs have revolutionized every industry and are also used in a wide range of applications for civil, commercial, and military purposes. UAVs are most commonly applied in the sectors displayed in Figure 3 and summarized in Table 9.

**Table 9.** Summary of applications.

Applications	References
<b>Mapping and surveying</b>	
Terrain mapping and modeling	[59,64,69–73]
Underground and surface karst areas	[6,74–79]
Mining	[80–86]
Real estate cadastre	[87–93]
Industry	[94–100]
Architecture	[101–107]
<b>Environmental activities</b>	
Agricultural	[108–114]
Forestry	[60,63,64,66,80,115]
Counting wild plants and animals	[117–123]
<b>Documentation of historical heritage</b>	
Documentation of historical monuments	[124–130]
Archaeology	[131–137]
<b>Natural hazards and geohazards</b>	
Geohazards	[58,138–142]
Volcano	[143–149]
Landslide	[150–156]
Stability of slopes	[157–163]
Geology	[164–170]
Hydrology	[171–177]
<b>Non-surveying applications</b>	
Aerial photography and videography	[73,178–180,182–184]
Search and rescue	[185–191]
Military	[192–197]
Checking electrical lines and pipes	[198–203]

### 6.3. Discussion on UAV Carriers, Sensors, and Software

We further divided the articles and literature that we studied in this publication according to the UAV carriers (Table 10), the type of sensor (Table 11), and the software that was used in data processing (Table 12). Most authors use the UAV DJI Phantom Pro for scientific purposes, but UAV DJI Phantom 4 and UAV DJI Mavic are also very common. Canon and Sony cameras are the most used digital cameras. The Velodyne lidar scanner is most commonly used for lidar data acquisition. Finally, the authors most often used Agisoft products and Pix4D software for data processing.

**Table 10.** Classification by UAV carrier.

UAV	References
DJI Phantom 4 Pro	[59,61,69,71,77,79,89,107,108,115,127,129,142,161,170,198]
DJI Phantom 4	[58,82,103,120,135,138,157]
DJI Phantom 3	[68,78,80,93,131,137,179]
DJI Phantom 2	[73,131,159,164]
DJI Mavic	[94,100,104,129,131,148,187]
DJI Matrice	[96,109,110,115,116,151]
DJI Inspire	[62,119,176]
3DR Solo	[60,105,120]
Droidworx Skyjib Oktokopter	[63,66]
DJI S1000	[81,88]

**Table 11.** Classification by sensor.

Sensor	Type of Sensor	References
Canon EOS	digital camera	[63,87,103,106,111,126,156]
Canon PowerShot	digital camera	[101,120,146,147,182]
Sony Alpha	digital camera	[125,132,135,150,165,177]
Sony EXMOR	digital camera	[68,93,168,179]
Sony ILCE	digital camera	[81,87,88]
DJI Phantom 4 integrated camera (12,4 MP)	digital camera	[58,82,103,120,135,138,157]
DJI Phantom 4 Pro integrated camera (20 MP)	digital camera	[59,61,69,71,77,79,89,107,108,115,127,129,142,161,170,198]
DJI Zenmuse	digital camera	[62,88,110,119,148,176]
Nikon	digital camera	[70,91,101,178,199]
GoPro	digital camera	[102,105,131,186,188]
Parrot Sequoia	multispectral camera	[59,60,64,69,190]
Panasonic	digital camera	[119,154]
Velodyne	lidar	[64,67,96,107,116]
Leica	lidar	[76,103,158]
Riegl VUX	lidar	[65,96,116]
Ibeo LUX	lidar	[63,66]
Odroid XU4	lidar	[109]
LiteMapper	lidar	[147]

**Table 12.** Classification by software.

Software	References
Pix4D	[77,79,82,104,107,137,168,177]
Agisoft Photoscan	[63,74,101,106,142,165]
Agisoft MetaShape	[58,61,62,74]
Autodesk, Autodesk ReCap	[104,106]
COLMAP	[106]
LiDAR360	[64,106]
QGIS	[137]
RiSCAN PRO	[101]

6.4. High-Frequency Keyword Analysis

For analysis of scientific studies filling the references of this review, 156 different research publications indexed in the Web of Science (WOS) were chosen. In total, 538 keywords were obtained, which were subject to further processing. The main themes of the analysis of the common occurrence of the keyword were the use and application of UAVs. The results of the systematic analysis of keywords helped us better understand the development and further direction of research in this field. With this approach, we wanted to identify the power of links between keywords and the number of analyzed documents. The same approach was also used by the authors Shi, J.-G. et al. [204]. Through the Vosviewer interface, the identified network of the common occurrence of keywords was divided into eight primary clusters (Figure 4). Each keyword in Figure 4 was visualized through one node using a colored visualization of circle symbols.

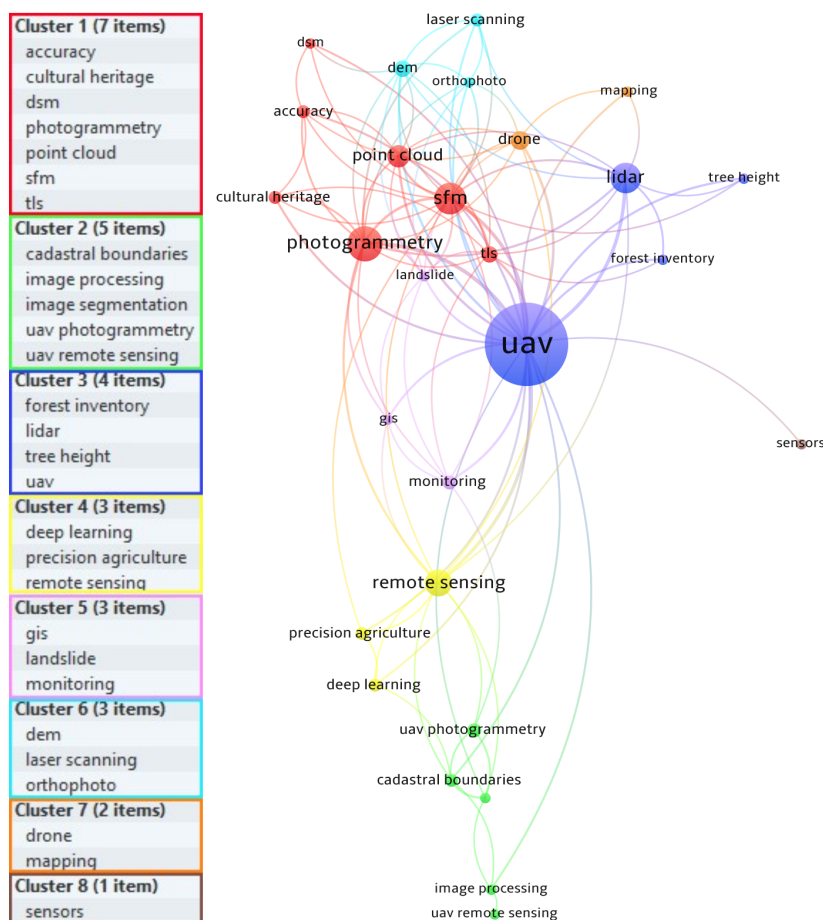


**Figure 4.** Co-occurrence network of high-frequency keywords with colored clusters.

The size of the node itself varies. It is expressed by a direct linear dependence on the number of keywords (larger symbols and text mean a higher occurrence of keywords). The choice of selection condition to recognize the keywords with a frequency of more than three appearances (threshold) was set in our study. The interconnection between two nodes creates/indicates a relationship between the specific keywords (Table 13).

**Table 13.** The keywords information of all clusters.

ID Number	Keywords	Occurrences	Total Link Strength
1	uav	89	112
2	photogrammetry	21	44
3	sfm	18	41
4	lidar	17	27
5	remote sensing	14	25
6	point cloud	10	17
7	drone	8	13
8	dem	6	13
9	tls	6	17
10	monitoring	5	10
11	uav photogrammetry	5	6
12	accuracy	4	10
13	cadastral boundaries	4	10
14	cultural heritage	4	8
15	deep learning	4	6
16	laser scanning	4	8
17	precision agriculture	4	8
18	dsm	3	5
19	forest inventory	3	6
20	gis	3	8
21	image processing	3	5
22	image segmentation	3	8
23	landslide	3	13
24	mapping	3	4
25	orthophoto	3	9
26	sensors	3	1
27	tree height	3	5
28	uav remote sensing	3	1

The processing interface identified 28 keywords (256 occurrences and a total link strength of 440 on UAVs). The results show that it is probable that there are other research areas related to the central term UAV. This result presents the conclusion that reflects the relationship between every important node, theme, and keyword. Circular nodes such as Photogrammetry, SfM, lidar, and Remote Sensing in UAV binding are the most significant and co-occurring, presenting a possible further direction in this research field.

## 7. Conclusions

This review has discussed and analyzed approaches for documenting, mapping, surveying, and monitoring diverse natural or artificial objects based on non-contact laser scanning and photogrammetric sensors on UAV carriers. Studies of terrain and land surface, buildings and technical objects, archeological and agricultural localities, and many other areas were included. The advantage of both methods is that they can quickly provide results with a large number of spatial data, with high accuracy and detail. The basic principles of laser scanning, photogrammetry, and the main principle of the SfM method, one of the most modern and advanced methods, were briefly explained. Nowadays, the use of non-contact methods using UAV vehicles is very popular. They are used for tracking and monitoring objects on the Earth's surface in many different applications and fields, such as research, military, agriculture, architecture, the monitoring of natural processes and phenomena, and commercial purposes. In this review, the principle of the operation of UAVs and the control of UAVs have been explained. When choosing the data collection method and the type of UAV, a surveyor must consider the size of the area to be mapped, the required point density, positional and height accuracy, the time required, and the cost. We have also addressed the advantages and disadvantages of using GCP points in surveying and using UAV with an on-board GNSS RTK/PPK module. In the next sections, we examined the use of UAV technology from a historical perspective and classified UAVs according to size, range and endurance, weight, wings, number of rotors, and purpose. The development of UAV technology also leads to its misuse, so in a separate section, we emphasized legislation and regulatory rules in selected countries. The last part of the article compared different types of UAVs in different specific conditions, with varying flight heights, types, and settings of sensors and environment. In addition, we compared the results based on GSD and RMSE.

In this review, we adopted the terminology according to [205], and we tried to adhere to it. In the literature cited in the text, the names of UAV carriers and sensors have been kept in their original notation.

**Author Contributions:** Conceptualization L.K., B.T., P.P. and P.B.; methodology L.K., B.T., P.P., M.B. and P.B.; software, L.K., B.T. and P.P.; validation, L.K., B.T., P.P., P.B. and M.B.G.; formal analysis, L.K., B.T., P.P., P.B. and M.B.G.; investigation, L.K.; resources B.T. and P.P.; data curation, L.K., B.T., M.B. and P.P.; writing—original draft preparation, L.K., B.T. and P.P.; writing—review and editing, L.K., B.T., P.P., P.B. and M.B.G.; visualization, L.K., B.T., P.P. and M.B.G.; supervision, L.K. All authors have read and agreed to the published version of the manuscript.

**Funding:** This research was supported by the Slovak Research and Development Agency under contract KEGA grant no. 055TUKE-4/2021, KEGA 003TUKE-4/2023 grant no. APVV-18-0351, APVV-20-0281, grant no. VEGA 1/0588/21, and project Mobile Monitoring System for the Protection of Isolated and Vulnerable Population Groups against Spread of Viral Diseases, ITMS code 313011AUP1, co-funded by the European Regional Development Fund under the Operational Programme Integrated Infrastructure.

**Institutional Review Board Statement:** Not applicable.

**Informed Consent Statement:** Not applicable.

**Data Availability Statement:** Not applicable.

**Conflicts of Interest:** The authors declare no conflict of interest.

## References

1. Wang, J.; Wang, L.; Jia, M.; He, Z.; Bi, L. Construction and optimization method of the open-pit mine DEM based on the oblique photogrammetry generated DSM. *Measurement* **2020**, *152*, 107322. [[CrossRef](#)]
2. Salach, A.; Bakuła, K.; Pilarska, M.; Ostrowski, W.; Górski, K.; Kurczyński, Z. Accuracy Assessment of Point Clouds from LiDAR and Dense Image Matching Acquired Using the UAV Platform for DTM Creation. *ISPRS Int. J. Geo-Inf.* **2018**, *7*, 342. [[CrossRef](#)]
3. Hofierka, J.; Gallay, M.; Bandura, P.; Šašák, J. Identification of karst sinkholes in a forested karst landscape using airborne laser scanning data and water flow analysis. *Geomorphology* **2018**, *308*, 265–277. [[CrossRef](#)]

4. Brede, B.; Lau, A.; Bartholomeus, H.M.; Kooistra, L. Comparing RIEGL RiCOPTER UAV LiDAR Derived Canopy Height and DBH with Terrestrial LiDAR. *Sensors* **2017**, *17*, 2371. [CrossRef]
5. Szabó, S.; Enyedi, P.; Horváth, M.; Kovács, Z.; Burai, P.; Csoknyai, T.; Szabó, G. Automated registration of potential locations for solar energy production with Light Detection And Ranging (LiDAR) and small format photogrammetry. *J. Clean. Prod.* **2016**, *112*, 3820–3829. [CrossRef]
6. Pukanská, K.; Bartoš, K.; Bella, P.; Gašinec, J.; Blistan, P.; Kovanič, L. Surveying and High-Resolution Topography of the Ochtiná Aragonite Cave Based on TLS and Digital Photogrammetry. *Appl. Sci.* **2020**, *10*, 4633. [CrossRef]
7. Blistan, P.; Jacko, S.; Kovanič, L.; Kondela, J.; Pukanská, K.; Bartoš, K. TLS and SfM Approach for Bulk Density Determination of Excavated Heterogeneous Raw Materials. *Minerals* **2020**, *10*, 174. [CrossRef]
8. Mlambo, R.; Woodhouse, I.H.; Gerard, F.; Anderson, K. Structure from Motion (SfM) Photogrammetry with Drone Data: A Low Cost Method for Monitoring Greenhouse Gas Emissions from Forests in Developing Countries. *Forests* **2017**, *8*, 68. [CrossRef]
9. Koska, B.; Křemen, T. The Combination of Laser Scanning and Structure from Motion Technology for Creation of Accurate Exterior and Interior Orthophotos of St. Nicholas Baroque Church. *ISPRS Int. Arch. Photogramm. Remote Sens. Spat. Inf. Sci.* **2013**, *40*, 133–138. [CrossRef]
10. Jiang, S.; Jiang, W. On-Board GNSS/IMU Assisted Feature Extraction and Matching for Oblique UAV Images. *Remote Sens.* **2017**, *9*, 813. [CrossRef]
11. Zeybek, M. Accuracy assessment of direct georeferencing UAV images with onboard global navigation satellite system and comparison of CORS/RTK surveying methods. *Meas. Sci. Technol.* **2021**, *32*, 065402. Available online: <https://iopscience.iop.org/article/10.1088/1361-6501/abf25d> (accessed on 1 January 2023). [CrossRef]
12. Štroner, M.; Urban, R.; Seidl, J.; Reindl, T.; Brouček, J. Photogrammetry Using UAV-Mounted GNSS RTK: Georeferencing Strategies without GCPs. *Remote Sens.* **2021**, *13*, 1336. [CrossRef]
13. Tomašík, J.; Mokroš, M.; Surový, P.; Grznárová, A.; Merganič, J. UAV RTK/PPK Method—An Optimal Solution for Mapping Inaccessible Forested Areas? *Remote Sens.* **2019**, *11*, 721. [CrossRef]
14. Forlani, G.; Dall’Asta, E.; Diotri, F.; Cella, U.M.d.; Roncella, R.; Santise, M. Quality Assessment of DSMs Produced from UAV Flights Georeferenced with On-Board RTK Positioning. *Remote Sens.* **2018**, *10*, 311. [CrossRef]
15. Kovanič, L.; Blišťan, P.; Štroner, M.; Urban, R.; Blišťanova, M. Suitability of Aerial Photogrammetry for Dump Documentation and Volume Determination in Large Areas. *Appl. Sci.* **2021**, *11*, 6564. [CrossRef]
16. Eltner, A.; Hoffmeister, D.; Kaiser, A.; Karrasch, P.; Klingbeil, L.; Stöcker, C.; Rovere, A. *UAVs for the Environmental Sciences: Methods and Applications*; Academic: Darmstadt/Berlin, Germany, 2022; ISBN 978-3-534-40588-6.
17. Archibald, D.F. An account of some preliminary experiments with Biram’s anemometers attached to kite strings or wires. *Nature* **1884**, *31*, 66–68.
18. McAdie, A. Atmospheric electricity at high altitudes. *Proc. Am. Acad. Arts Sci.* **1885**, *21*, 129–134. [CrossRef]
19. Operator’s Guidance for Drone Pilots. European Union Aviation Safety Agency [Online]. Available online: <https://www.easa.europa.eu/en/light/topics/operators-guidance-drone-pilots> (accessed on 1 January 2023).
20. Pravidlá Používania Dronov. MAM DRON. Available online: <https://mamdron.sk/legislativa/> (accessed on 1 January 2023).
21. Abdullah, Q. Classification of the Unmanned Aerial Systems. In *Geospatial Applications of Unmanned Aerial Systems (UAS)*; PennState College of Earth and Mineral Science: University Park, PA, USA, 2020; Available online: <https://www.e-education.psu.edu/geog892/node/5> (accessed on 1 January 2023).
22. Eisenbeiss, H. UAV Photogrammetry. Ph.D. Thesis, Institut für Geodäsie und Photogrammetrie, Eidgenössische Technische Hochschule, Zürich, Switzerland, 2009.
23. Rennie, J. Drone Types: Multi-Rotor vs. Fixed-Wing vs. Single Rotor vs. Hybrid Vtol. AUAV. 2016. Available online: <https://www.auav.com.au/articles/drone-types/> (accessed on 1 January 2023).
24. Different Types of Survey Drones and How They Take Off, Fly and Land. Position Partners. Available online: <https://www.positionpartners.com.au/position-partners/survey-drones/> (accessed on 1 January 2023).
25. Guan, S.; Zhu, Z.; Wang, G. A Review on UAV-Based Remote Sensing Technologies for Construction and Civil Applications. *Drones* **2022**, *6*, 117. [CrossRef]
26. Lee, S.; Choi, Y. Reviews of unmanned aerial vehicle (drone) technology trends and its applications in the mining industry. *Geosystem Eng.* **2016**, *19*, 197–204. Available online: <https://www.tandfonline.com/doi/full/10.1080/12269328.2016.1162115> (accessed on 1 January 2023). [CrossRef]
27. Lyu, X.; Li, X.; Dang, D.; Dou, H.; Wang, K.; Lou, A. Unmanned Aerial Vehicle (UAV) Remote Sensing in Grassland Ecosystem Monitoring: A Systematic Review. *Remote Sens.* **2022**, *14*, 1096. [CrossRef]
28. Crommelinck, S.; Bennett, R.; Gerke, M.; Nex, F.; Yang, M.Y.; Vosselman, G. Review of Automatic Feature Extraction from High-Resolution Optical Sensor Data for UAV-Based Cadastral Mapping. *Remote Sens.* **2016**, *8*, 689. [CrossRef]
29. The European Commission. Commission Implementing Regulation (EU) 2019/947 of 24 May 2019 on the Rules and Procedures for the Operation of Unmanned Aircraft. Official Journal of the European Union 2019, L 152/45. Available online: <https://eur-lex.europa.eu/legal-content/EN/TXT/?uri=CELEX%3A32019R0947> (accessed on 1 January 2023).
30. Kacvinský, A. Pravidlá Lietania s Dronmi 2022 | EU Legislatíva. APROP. Available online: <https://www.aprop.sk/clanok/legislativa-pravidla-lietanie-drony/> (accessed on 1 January 2023).

31. DOPRAVNÝ ÚRAD. Lietadlá Spôsobilé Lietat' bez Pilota (Bezpilotné Lietadlá). Available online: <http://letectvo.nsat.sk/letova-prevadzka/lietadla-sposobile-lietat-bez-pilota/> (accessed on 1 January 2023).
32. LPS, S.R. Elektronický VFR Manuál. Available online: <https://gis.lps.sk/vfrm/index.html> (accessed on 2 January 2023).
33. Národná Rada Slovenskej Republiky. ZÁKON č. 143/1998 Z. z. z 2. Apríla 1998 o Civilnom Letectve (Letecký Zákon) a o Zmene a Doplnení Niektorých Zákonov. Zbierka Zákonov Slovenskej Republiky. 2021. Available online: <https://www.slov-lex.sk/pravne-predpisy/SK/ZZ/1998/143/20211101> (accessed on 2 January 2023).
34. Ústredný Kontrolný a Skúšobný Ústav Poľnohospodársky. Letecké Aplikácie. Available online: <https://www.uksup.sk/oor-letecke-aplikacie> (accessed on 4 January 2023).
35. ÚŘAD PRO CIVILNÍ LETECTVÍ. Bezpilotní Letadla. Available online: <https://www.caa.cz/provoz/bezpilotni-letadla/> (accessed on 4 January 2023).
36. Řízení Letového Provozu. Létejte Zodpovědně. Available online: <https://letejtezodpovedne.cz/> (accessed on 4 January 2023).
37. Dronetag. Dronald. Available online: <https://www.dronald.cz/> (accessed on 5 January 2023).
38. Řízení Letového Provozu. Bezpilotní Létání. Available online: <https://www.rlp.cz/categorysb?CatCode=C3> (accessed on 5 January 2023).
39. Řízení Letového Provozu. AisView. Available online: <https://dronview.rlp.cz/> (accessed on 5 January 2023).
40. Česká Národní Rada. ZÁKON č. 49/1997 Sb., ze dne 6. Března 1997 o Civilním Letectví a o Změně a Doplnění Zákona č. 455/1991 Sb., o Živnostenském Podnikání (Živnostenský Zákon), ve Znění Pozdějších Předpisů. Sbirka Zákonů České Republiky. Available online: [https://aplikace.mvcr.cz/sbirka-zakonu/SearchResult.aspx?q=49/1997&typeLaw=zakon&what=Cislo\\_zakona\\_smlouvy](https://aplikace.mvcr.cz/sbirka-zakonu/SearchResult.aspx?q=49/1997&typeLaw=zakon&what=Cislo_zakona_smlouvy) (accessed on 5 January 2023).
41. Urząd Lotnictwa Cywilnego. Bezzałogowe Statki Powietrzne. Available online: <https://www.ulc.gov.pl/pl/drony> (accessed on 5 January 2023).
42. UAV COACH. Drone Laws in Poland. Available online: <https://uavcoach.com/drone-laws-in-poland/> (accessed on 7 January 2023).
43. PANSÁ. Poznaj PansaUTM. Available online: <https://www.pansa.pl/poznaj-pansautm/> (accessed on 9 January 2023).
44. Dlapilota.pl. DroneRadar. Available online: <https://droneradar.eu/> (accessed on 9 January 2023).
45. Technológiai és Ipari Minisztérium. Közlekedési Hatóság. Available online: <https://www.kozlekedesihatosag.kormany.hu/hu/web/guest/a-hatosagrol> (accessed on 9 January 2023).
46. Propelrc. Every Drone Laws in Hungary (2023 Updated). Available online: <https://www.propelrc.com/drone-laws-in-hungary/> (accessed on 12 January 2023).
47. DroneLaws. Drone Laws in Hungary. Available online: <https://drone-laws.com/drone-laws-in-hungary/> (accessed on 12 January 2023).
48. LÉGTÉR. Térkép. Available online: <https://terkep.legter.hu/#7/47.2/19.5> (accessed on 12 January 2023).
49. AUSTRO CONTROL. DRONESPACE. Available online: <https://www.dronespace.at/> (accessed on 14 January 2023).
50. UAV COACH. Drone Laws in Austria. Available online: <https://uavcoach.com/drone-laws-in-austria/> (accessed on 18 January 2023).
51. AUSTRO CONTROL. Bewilligung UAS-Betrieb Sicherheitszone. Available online: <https://dronespace.at/jart/prj3/dronespace/data/uploads/Bewilligung%20UAS-Betrieb%20Sicherheitszone.pdf> (accessed on 18 January 2023).
52. AUSTRO CONTROL. Bewilligung UAS-Betrieb Flugbeschränkungsgebiet. Available online: [https://dronespace.at/jart/prj3/dronespace/data/uploads/FO\\_LFA\\_DCC\\_010\\_DE.pdf](https://dronespace.at/jart/prj3/dronespace/data/uploads/FO_LFA_DCC_010_DE.pdf) (accessed on 18 January 2023).
53. AUSTRO CONTROL. Drone Space App. Available online: <https://map.dronespace.at/> (accessed on 18 January 2023).
54. Luftfahrt-Bundesamt. Drohnen. Available online: [https://www.lba.de/DE/Drohnen/Drohnen\\_node.html](https://www.lba.de/DE/Drohnen/Drohnen_node.html) (accessed on 20 January 2023).
55. UAV COACH. Drone Laws in Germany. Available online: <https://uavcoach.com/drone-laws-in-germany/> (accessed on 20 January 2023).
56. FlyNex. Map. Available online: <https://app.flynex.io/a/map/fn> (accessed on 21 January 2023).
57. Digitale Plattform Unbemannte Luftfahrt. Map Tool. Available online: <https://maptool-dipul.dfs.de/?language=de> (accessed on 21 January 2023).
58. Kovanič, L.; Blistan, P.; Urban, R.; Štroner, M.; Blišťanová, M.; Bartoš, K.; Pukanská, K. Analysis of the Suitability of High-Resolution DEM Obtained Using ALS and UAS (SfM) for the Identification of Changes and Monitoring the Development of Selected Geohazards in the Alpine Environment—A Case Study in High Tatras, Slovakia. *Remote Sens.* **2020**, *12*, 3901. [CrossRef]
59. Guan, S.; Fukami, K.; Matsunaka, H.; Okami, M.; Tanaka, R.; Nakano, H.; Sakai, T.; Nakano, K.; Ohdan, H.; Takahashi, K. Assessing Correlation of High-Resolution NDVI with Fertilizer Application Level and Yield of Rice and Wheat Crops Using Small UAVs. *Remote Sens.* **2019**, *11*, 112. [CrossRef]
60. Johansen, K.; Raharjo, T.; McCabe, M.F. Using Multi-Spectral UAV Imagery to Extract Tree Crop Structural Properties and Assess Pruning Effects. *Remote Sens.* **2018**, *10*, 854. [CrossRef]
61. Vanneschi, C.; Di Camillo, M.; Aiello, E.; Bonciani, F.; Salvini, R. SfM-MVS Photogrammetry for Rockfall Analysis and Hazard Assessment Along the Ancient Roman Via Flaminia Road at the Furlo Gorge (Italy). *ISPRS Int. J. Geo-Inf.* **2019**, *8*, 325. [CrossRef]
62. Moe, K.T.; Owari, T.; Furuya, N.; Hiroshima, T. Comparing Individual Tree Height Information Derived from Field Surveys, LiDAR and UAV-DAP for High-Value Timber Species in Northern Japan. *Forests* **2020**, *11*, 223. [CrossRef]

63. Wallace, L.; Lucieer, A.; Malenovský, Z.; Turner, D.; Vopěnka, P. Assessment of Forest Structure Using Two UAV Techniques: A Comparison of Airborne Laser Scanning and Structure from Motion (SfM) Point Clouds. *Forests* **2016**, *7*, 62. [[CrossRef](#)]
64. Cao, L.; Liu, H.; Fu, X.; Zhang, Z.; Shen, X.; Ruan, H. Comparison of UAV LiDAR and Digital Aerial Photogrammetry Point Clouds for Estimating Forest Structural Attributes in Subtropical Planted Forests. *Forests* **2019**, *10*, 145. [[CrossRef](#)]
65. D'hont, B.; Calders, K.; Bartholomeus, H.; Whiteside, T.; Bartolo, R.; Levick, S.; Krishna Moorthy, S.M.; Terry, L.; Verbeeck, H. Characterising Termite Mounds in a Tropical Savanna with UAV Laser Scanning. *Remote Sens.* **2021**, *13*, 476. [[CrossRef](#)]
66. Wallace, L.; Lucieer, A.; Watson, C.; Turner, D. Development of a UAV-LiDAR System with Application to Forest Inventory. *Remote Sens.* **2012**, *4*, 1519–1543. [[CrossRef](#)]
67. Glennie, C.; Brooks, B.; Ericksen, T.; Hauser, D.; Hudnut, K.; Foster, J.; Avery, J. Compact Multipurpose Mobile Laser Scanning System—Initial Tests and Results. *Remote Sens.* **2013**, *5*, 521–538. [[CrossRef](#)]
68. Crommelinck, S.; Bennett, R.; Gerke, M.; Yang, M.Y.; Vosselman, G. Contour Detection for UAV-Based Cadastral Mapping. *Remote Sens.* **2017**, *9*, 171. [[CrossRef](#)]
69. Yang, B.; Hawthorne, T.L.; Torres, H.; Feinman, M. Using Object-Oriented Classification for Coastal Management in the East Central Coast of Florida: A Quantitative Comparison between UAV, Satellite, and Aerial Data. *Drones* **2019**, *3*, 60. [[CrossRef](#)]
70. Wen, D.; Su, L.; Hu, Y.; Xiong, Z.; Liu, M.; Long, Y. Surveys of Large Waterfowl and Their Habitats Using an Unmanned Aerial Vehicle: A Case Study on the Siberian Crane. *Drones* **2021**, *5*, 102. [[CrossRef](#)]
71. Tucci, G.; Gebbia, A.; Conti, A.; Fiorini, L.; Lubello, C. Monitoring and Computation of the Volumes of Stockpiles of Bulk Material by Means of UAV Photogrammetric Surveying. *Remote Sens.* **2019**, *11*, 1471. [[CrossRef](#)]
72. Zanutta, A.; Lambertini, A.; Vittuari, L. UAV Photogrammetry and Ground Surveys as a Mapping Tool for Quickly Monitoring Shoreline and Beach Changes. *J. Mar. Sci. Eng.* **2020**, *8*, 52. [[CrossRef](#)]
73. Santano, D.; Esmaili, H. Aerial videography in built heritage documentation: The case of Post-Independence Architecture of Malaysia. In Proceedings of the 2014 International Conference on Virtual Systems & Multimedia (VSMM), Hong Kong, China, 9–12 December 2014; pp. 323–328. [[CrossRef](#)]
74. Szczygieł, J.; Golicz, M.; Hercman, H.; Lynch, E. Geological constraints on cave development in the plateau-gorge karst of South China (Wulong, Chongqing). *Geomorphology* **2018**, *304*, 50–63. [[CrossRef](#)]
75. Bella, P.; Bosák, P.; Pruner, P.; Hercman, H.; Pukanská, K.; Bartoš, K.; Gaál, L.; Haviarová, D.; Tomčík, P.; Kdýr, Š. Speleogenesis in a lens of metamorphosed limestone and ankerite: Ochtiná Aragonite Cave, Slovakia. *Int. J. Speleol.* **2022**, *51*, 13–28. [[CrossRef](#)]
76. Hofierka, J.; Gallay, M.; Kaňuk, J.; Šašák, J. Modelling Karst Landscape with Massive Airborne and Terrestrial Laser Scanning Data. In *The Rise of Big Spatial Data. Lecture Notes in Geoinformation and Cartography*; Ivan, I., Singleton, A., Horák, J., Inspektor, T., Eds.; Springer: Cham, Switzerland, 2017.
77. Li, Y.; Deng, T.; Fu, B.; Lao, Z.; Yang, W.; He, H.; Fan, D.; He, W.; Yao, Y. Evaluation of Decision Fusions for Classifying Karst Wetland Vegetation Using One-Class and Multi-Class CNN Models with High-Resolution UAV Images. *Remote Sens.* **2022**, *14*, 5869. [[CrossRef](#)]
78. Xu, A.A.; Wang, F.; Li, L. Vegetation information extraction in karst area based on UAV remote sensing in visible light band. *Optik* **2023**, *272*, 170355. [[CrossRef](#)]
79. Yang, S.T.; Li, C.J.; Lou, H.Z.; Wang, P.F.; Wu, X.J.; Zhang, Y.C.; Zhang, J.; Li, X. Role of the countryside landscapes for sustaining biodiversity in karst areas at a semi centennial scale. *Ecol. Indic.* **2021**, *123*, 107315. [[CrossRef](#)]
80. Park, S.; Choi, Y. Applications of Unmanned Aerial Vehicles in Mining from Exploration to Reclamation: A Review. *Minerals* **2020**, *10*, 663. [[CrossRef](#)]
81. Ćwiąkała, P.; Gruszczynski, W.; Stoch, T.; Puniach, E.; Mrocheń, D.; Matwij, W.; Matwij, K.; Nędzka, M.; Sopata, P.; Wójcik, A. UAV Applications for Determination of Land Deformations Caused by Underground Mining. *Remote Sens.* **2020**, *12*, 1733. [[CrossRef](#)]
82. Fernández-Lozano, J.; González-Díez, A.; Gutiérrez-Alonso, G.; Carrasco, R.M.; Pedraza, J.; García-Talegón, J.; Alonso-Gavilán, G.; Remondo, J.; Bonachea, J.; Morellón, M. New Perspectives for UAV-Based Modelling the Roman Gold Mining Infrastructure in NW Spain. *Minerals* **2018**, *8*, 518. [[CrossRef](#)]
83. Ge, L.; Li, X.; Ng, A.H.M. UAV for mining applications: A case study at an open-cut mine and a longwall mine in New South Wales, Australia. In Proceedings of the 2016 IEEE International Geoscience and Remote Sensing Symposium (IGARSS), Beijing, China, 10–15 July 2016; pp. 5422–5425. [[CrossRef](#)]
84. Chen, J.; Li, K.; Chang, K.-J.; Soa, G.; Tarolli, P. Open-pit mining geomorphic feature characterisation. *Int. J. Appl. Earth Obs. Geoinf.* **2015**, *42*, 76–86. [[CrossRef](#)]
85. Ren, H.; Zhao, Y.; Xiao, W.; Hu, Z. A review of UAV monitoring in mining areas: Current status and future perspectives. *Int. J. Coal Sci. Technol.* **2019**, *6*, 320–333. [[CrossRef](#)]
86. Chen, J.; Li, K.; Chang, K.-J.; Sofia, G.; Tarolli, P. Open-pit mine geomorphic changes analysis using multi-temporal UAV survey. *Environ. Earth Sci.* **2018**, *77*, 220. [[CrossRef](#)]
87. Šafář, V.; Potůčková, M.; Karas, J.; Thustý, J.; Štefanová, E.; Jančovič, M.; Cígler Žofková, D. The Use of UAV in Cadastral Mapping of the Czech Republic. *ISPRS Int. J. Geo-Inf.* **2021**, *10*, 380. [[CrossRef](#)]
88. Puniach, E.; Bieda, A.; Ćwiąkała, P.; Kwartnik-Pruc, A.; Parzych, P. Use of Unmanned Aerial Vehicles (UAVs) for Updating Farmland Cadastral Data in Areas Subject to Landslides. *ISPRS Int. J. Geo-Inf.* **2018**, *7*, 331. [[CrossRef](#)]

89. Fetai, B.; Oštir, K.; Kosmatin Fras, M.; Lisec, A. Extraction of Visible Boundaries for Cadastral Mapping Based on UAV Imagery. *Remote Sens.* **2019**, *11*, 1510. [[CrossRef](#)]
90. Chio, S.-H.; Chiang, C.-C. Feasibility Study Using UAV Aerial Photogrammetry for a Boundary Verification Survey of a Digitalized Cadastral Area in an Urban City of Taiwan. *Remote Sens.* **2020**, *12*, 1682. [[CrossRef](#)]
91. Rokhmana, C.A.; Utomo, S. The Low-Cost UAV-Based Remote Sensing System Capabilities for Large Scale Cadaster Mapping. *IOP Conf. Ser. Earth Environ. Sci.* **2016**, *47*, 012005. [[CrossRef](#)]
92. Xia, X.; Koeva, M.; Persello, C. Extracting cadastral boundaries from uav images using fully convolutional networks. In Proceedings of the IGARSS 2019-2019 IEEE International Geoscience and Remote Sensing Symposium, Yokohama, Japan, 28 July–2 August 2019; pp. 2455–2458. [[CrossRef](#)]
93. Yuwono, B.D.; Suprayogi, A.; Azeriansyah, R.; Nukita, D. UAV Photogrammetry Implementation Based on GNSS CORS UDIP to Enhance Cadastral Surveying and Monitoring Urban Development (Case Study: Ngresep Semarang). *IOP Conf. Ser. Earth Environ. Sci.* **2018**, *165*, 012031. [[CrossRef](#)]
94. Ajayi, O.G.; Ajulo, J. Investigating the Applicability of Unmanned Aerial Vehicles (UAV) Photogrammetry for the Estimation of the Volume of Stockpiles. *Quaest. Geogr.* **2021**, *40*, 25–38. [[CrossRef](#)]
95. Cho, J.; Lim, G.; Biobaku, T.; Kim, S.; Parsaei, H. Safety and security management with unmanned aerial vehicle (UAV) in oil and gas industry. *Procedia Manuf.* **2015**, *3*, 1343–1349. [[CrossRef](#)]
96. Asadzadeh, S.; de Oliveira, W.J.; de Souza Filho, C.R. UAV-based remote sensing for the petroleum industry and environmental monitoring: State-of-the-art and perspectives. *J. Pet. Sci. Eng.* **2022**, *208*, 109633. [[CrossRef](#)]
97. Kim, D.H.; Lee, B.K.; Sohn, S.Y. Quantifying technology–industry spillover effects based on patent citation network analysis of unmanned aerial vehicle (UAV). *Technol. Forecast. Soc. Change* **2016**, *105*, 140–157. [[CrossRef](#)]
98. Lee, G.; Saad, W.; Bennis, M. Online Optimization for UAV-Assisted Distributed Fog Computing in Smart Factories of Industry 4.0. In Proceedings of the 2018 IEEE Global Communications Conference (GLOBECOM), Abu Dhabi, United Arab Emirates, 9–13 December 2018; pp. 1–6. [[CrossRef](#)]
99. Masduzzaman, M.; Nugraha, R.; Shin, S.Y. IoT-based CO<sub>2</sub> Gas-level Monitoring and Automated Decision-making System in Smart Factory using UAV-assisted MEC. In Proceedings of the 2022 International Conference on Decision Aid Sciences and Applications (DASA), Chiangrai, Thailand, 23–25 March 2022; pp. 1023–1027. [[CrossRef](#)]
100. Martín-Béjar, S.; Claver, J.; Sebastián, M.A.; Sevilla, L. Graphic Applications of Unmanned Aerial Vehicles (UAVs) in the Study of Industrial Heritage Assets. *Appl. Sci.* **2020**, *10*, 8821. [[CrossRef](#)]
101. Maiellaro, N.; Zonno, M.; Lavalle, P. Laser scanner and camera-equipped UAV architectural surveys. In *ISPRS International Archives of the Photogrammetry, Remote Sensing and Spatial Information Sciences*; XL-5; Copernicus Publications: Göttingen, Germany, 2015; pp. 381–386. [[CrossRef](#)]
102. Jutzi, B.; Weinmann, M.; Meidow, J. Weighted data fusion for UAV-borne 3D mapping with camera and line laser scanner. *Int. J. Image Data Fusion* **2014**, *5*, 226–243. [[CrossRef](#)]
103. Sun, Z.; Zhang, Y. Using Drones and 3D Modeling to Survey Tibetan Architectural Heritage: A Case Study with the Multi-Door Stupa. *Sustainability* **2018**, *10*, 2259. [[CrossRef](#)]
104. Lin, G.; Sang, K. Application of UAV-Based Oblique Photography in Architectural Design: The Case of Mengyuan Resort Hotel in Yunnan, China. In Proceedings of the 2021 4th International Conference on Civil Engineering and Architecture, Seoul, Republic of Korea, 10–12 July 2021; Kang, T., Lee, Y., Eds.; Lecture Notes in Civil Engineering. Springer: Singapore, 2022; Volume 201. [[CrossRef](#)]
105. Yastikli, N.; Özerdem, Ö.Z. Architectural Heritage Documentation by Using Low Cost Uav with Fisheye Lens: Otag-I Humayun in Istanbul as a Case Study. *ISPRS Ann. Photogramm. Remote Sens. Spatial Inf. Sci.* **2017**, *IV-4/W4*, 415–418. [[CrossRef](#)]
106. Germanese, D.; Leone, G.R.; Moroni, D.; Pascali, M.A.; Tampucci, M. Towards Structural Monitoring and 3D Documentation of Architectural Heritage Using UAV. In *Multimedia and Network Information Systems*; Choroś, K., Kopel, M., Kukla, E., Siemiński, A., Eds.; MISSI 2018. Advances in Intelligent Systems and Computing; Springer: Cham, Switzerland, 2019; Volume 833. [[CrossRef](#)]
107. Raman, M.G.; Carlos, E.F.; Sankaran, S. Optimization and Evaluation of Sensor Angles for Precise Assessment of Architectural Traits in Peach Trees. *Sensors* **2022**, *22*, 4619. [[CrossRef](#)]
108. Wei, Z.; Han, Y.; Li, M.; Yang, K.; Yang, Y.; Luo, Y.; Ong, S.-H. A Small UAV Based Multi-Temporal Image Registration for Dynamic Agricultural Terrace Monitoring. *Remote Sens.* **2017**, *9*, 904. [[CrossRef](#)]
109. Christiansen, M.P.; Laursen, M.S.; Jørgensen, R.N.; Skovsen, S.; Gislum, R. Designing and Testing a UAV Mapping System for Agricultural Field Surveying. *Sensors* **2017**, *17*, 2703. [[CrossRef](#)]
110. Lambertini, A.; Mandanici, E.; Tini, M.A.; Vittuari, L. Technical Challenges for Multi-Temporal and Multi-Sensor Image Processing Surveyed by UAV for Mapping and Monitoring in Precision Agriculture. *Remote Sens.* **2022**, *14*, 4954. [[CrossRef](#)]
111. Sona, G.; Passoni, D.; Pinto, L.; Pagliari, D.; Masseroni, D.; Ortuani, B.; Facchi, A. UAV Multispectral Survey to Map Soil and Crop for Precision Farming Applications. *ISPRS-Int. Arch. Photogramm. Remote Sens. Spat. Inf. Sci.* **2016**, *41*, 1023–1029. [[CrossRef](#)]
112. Yan, X.; Zhou, Y.; Liu, X.; Yang, D.; Yuan, H. Minimizing Occupational Exposure to Pesticide and Increasing Control Efficacy of Pests by Unmanned Aerial Vehicle Application on Cowpea. *Appl. Sci.* **2021**, *11*, 9579. [[CrossRef](#)]
113. Ahmed, S.; Qiu, B.; Ahmad, F.; Kong, C.-W.; Xin, H. A State-of-the-Art Analysis of Obstacle Avoidance Methods from the Perspective of an Agricultural Sprayer UAV's Operation Scenario. *Agronomy* **2021**, *11*, 1069. [[CrossRef](#)]

114. Bischoff, V.; Farias, K.; Menzen, J.P.; Pessin, G. Technological support for detection and prediction of plant diseases: A systematic mapping study. *Comput. Electron. Agric.* **2021**, *181*, 105922. [[CrossRef](#)]
115. Hartley, R.J.L.; Leonardo, E.M.; Massam, P.; Watt, M.S.; Estarija, H.J.; Wright, L.; Melia, N.; Pearse, G.D. An Assessment of High-Density UAV Point Clouds for the Measurement of Young Forestry Trials. *Remote Sens.* **2020**, *12*, 4039. [[CrossRef](#)]
116. Hu, T.; Sun, X.; Su, Y.; Guan, H.; Sun, Q.; Kelly, M.; Guo, Q. Development and Performance Evaluation of a Very Low-Cost UAV-Lidar System for Forestry Applications. *Remote Sens.* **2021**, *13*, 77. [[CrossRef](#)]
117. Osco, L.P.; dos S de Arruda, M.; Gonçalves, D.N.; Dias, A.; Batistoti, J.; de Souza, M.; Gomes, F.D.G.; Ramos, A.P.M.; de Castro Jorge, L.A.; Liesenberg, V.; et al. A CNN Approach to simultaneously count plants and detect plantation-rows from UAV imagery. *ISPRS J. Photogramm. Remote Sens.* **2021**, *174*, 1–17. [[CrossRef](#)]
118. Fuentes-Peñailillo, F.; Ortega-Farías, S.; de la Fuente-Sáiz, L.; Rivera, M. Digital count of Sunflower plants at emergence from very low altitude using UAV images. In Proceedings of the 2019 IEEE CHILEAN Conference on Electrical, Electronics Engineering, Information and Communication Technologies (CHILECON), Valparaiso, Chile, 13–27 November 2019; pp. 1–5. [[CrossRef](#)]
119. Machefer, M.; Lemarchand, F.; Bonnefond, V.; Hitchins, A.; Sidiropoulos, P. Mask R-CNN Refitting Strategy for Plant Counting and Sizing in UAV Imagery. *Remote Sens.* **2020**, *12*, 3015. [[CrossRef](#)]
120. García-Martínez, H.; Flores-Magdaleno, H.; Khalil-Gardezi, A.; Ascencio-Hernández, R.; Tijerina-Chávez, L.; Vázquez-Peña, M.A.; Mancilla-Villa, O.R. Digital Count of Corn Plants Using Images Taken by Unmanned Aerial Vehicles and Cross Correlation of Templates. *Agronomy* **2020**, *10*, 469. [[CrossRef](#)]
121. Lee, S.; Song, Y.; Kil, S.-H. Feasibility Analyses of Real-Time Detection of Wildlife Using UAV-Derived Thermal and RGB Images. *Remote Sens.* **2021**, *13*, 2169. [[CrossRef](#)]
122. Dundas, S.J.; Vardanega, M.; O'Brien, P.; McLeod, S.R. Quantifying Waterfowl Numbers: Comparison of Drone and Ground-Based Survey Methods for Surveying Waterfowl on Artificial Waterbodies. *Drones* **2021**, *5*, 5. [[CrossRef](#)]
123. Barbedo, J.G.A.; Koenigkan, L.V.; Santos, P.M.; Ribeiro, A.R.B. Counting Cattle in UAV Images—Dealing with Clustered Animals and Animal/Background Contrast Changes. *Sensors* **2020**, *20*, 2126. [[CrossRef](#)]
124. Křemen, T. Measurement and documentation of St. Spirit Church in Liběchov. In *Advances and Trends in Geodesy, Cartography and Geoinformatics II*; CRC Press: Boca Raton, FL, USA, 2020; pp. 44–49. ISBN 978-0-367-34651-5.
125. Krátký, V.; Petráček, P.; Nascimento, T.; Čadilová, M.; Škobrtal, M.; Stoudek, P.; Saska, M. Safe Documentation of Historical Monuments by an Autonomous Unmanned Aerial Vehicle. *ISPRS Int. J. Geo-Inf.* **2021**, *10*, 738. [[CrossRef](#)]
126. Xu, Z.; Wu, L.; Shen, Y.; Li, F.; Wang, Q.; Wang, R. Tridimensional Reconstruction Applied to Cultural Heritage with the Use of Camera-Equipped UAV and Terrestrial Laser Scanner. *Remote Sens.* **2014**, *6*, 10413–10434. [[CrossRef](#)]
127. Orihuela, A.; Molina-Fajardo, M.A. UAV Photogrammetry Surveying for Sustainable Conservation: The Case of Mondújar Castle (Granada, Spain). *Sustainability* **2021**, *13*, 24. [[CrossRef](#)]
128. Petráček, P.; Krátký, V.; Saska, M. Dronument: System for Reliable Deployment of Micro Aerial Vehicles in Dark Areas of Large Historical Monuments. In *IEEE Robotics and Automation Letters*; IEEE: Piscataway, NJ, USA, 2020; Volume 5, pp. 2078–2085. [[CrossRef](#)]
129. Mulahusić, A.; Gajski, D.; Tuno, N.; Topoljak, J.; Đideliija, M.; Čatić, J.; Kogoj, D. Quality Evaluation of 3D Heritage Monument Models Derived from Images Obtained with Different Low-Cost Unmanned Aerial Vehicles. *Geod. List.* **2022**, *76*, 7–23. Available online: <https://hrcak.srce.hr/275234> (accessed on 1 January 2023).
130. Saponaro, M.; Capolupo, A.; Turso, A.; Tarantino, E. Cloud-to-cloud assessment of UAV and TLS 3D reconstructions of cultural heritage monuments: The case of Torre Zozzoli. In Proceedings of the Eighth International Conference on Remote Sensing and Geoinformation of the Environment (RSCy2020), Paphos, Cyprus, 16–18 March 2020; p. 1152408. [[CrossRef](#)]
131. Fiz, J.I.; Martín, P.M.; Cuesta, R.; Subías, E.; Codina, D.; Cartes, A. Examples and Results of Aerial Photogrammetry in Archeology with UAV: Geometric Documentation, High Resolution Multispectral Analysis, Models and 3D Printing. *Drones* **2022**, *6*, 59. [[CrossRef](#)]
132. Mesas-Carrascosa, F.-J.; Notario García, M.D.; Meroño de Larriva, J.E.; García-Ferrer, A. An Analysis of the Influence of Flight Parameters in the Generation of Unmanned Aerial Vehicle (UAV) Orthomosaics to Survey Archaeological Areas. *Sensors* **2016**, *16*, 1838. [[CrossRef](#)]
133. Schroder, W.; Murtha, T.; Golden, C.; Scherer, A.K.; Broadbent, E.N.; Almeyda Zambrano, A.M.; Herndon, K.; Griffin, R. UAV LiDAR Survey for Archaeological Documentation in Chiapas, Mexico. *Remote Sens.* **2021**, *13*, 4731. [[CrossRef](#)]
134. Ulvi, A. Using UAV Photogrammetric Technique for Monitoring, Change Detection, and Analysis of Archeological Excavation Sites. *J. Comput. Cult. Herit.* **2022**, *15*, 1–19. [[CrossRef](#)]
135. Tariq, A.; Gillani, S.M.O.A.; Qureshi, H.K.; Haneef, I. Heritage preservation using aerial imagery from light weight low cost Unmanned Aerial Vehicle (UAV). In Proceedings of the 2017 International Conference on Communication Technologies (ComTech), Rawalpindi, Pakistan, 19–21 April 2017; pp. 201–205. [[CrossRef](#)]
136. Balsi, M.; Esposito, S.; Fallavollita, P.; Melis, M.G.; Milanese, M. Preliminary Archeological Site Survey by UAV-Borne Lidar: A Case Study. *Remote Sens.* **2021**, *13*, 332. [[CrossRef](#)]
137. Gennaro, A.; Mangiameli, M.; Muscato, G.; Mussumeci, G.; Sgarlata, M. Geomatic techniques for surveying and mapping an archaeological site. In Proceedings of the 2018 Metrology for Archaeology and Cultural Heritage (MetroArchaeo), Cassino, Italy, 22–24 October 2018; pp. 277–281. [[CrossRef](#)]

138. Urban, R.; Štroner, M.; Blistan, P.; Kovanič, L.; Patera, M.; Jacko, S.; Ďuriška, I.; Kelemen, M.; Szabo, S. The Suitability of UAS for Mass Movement Monitoring Caused by Torrential Rainfall—A Study on the Talus Cones in the Alpine Terrain in High Tatras, Slovakia. *ISPRS Int. J. Geo-Inf.* **2019**, *8*, 317. Available online: <https://www.mdpi.com/2220-9964/8/8/317> (accessed on 1 January 2023). [[CrossRef](#)]
139. Yang, Y.-H.; Xu, Q.; Hu, J.-C.; Wang, Y.-S.; Dong, X.-J.; Chen, Q.; Zhang, Y.-J.; Li, H.-L. Source Model and Triggered Aseismic Faulting of the 2021 Mw 7.3 Maduo Earthquake Revealed by the UAV-Lidar/Photogrammetry, InSAR, and Field Investigation. *Remote Sens.* **2022**, *14*, 5859. [[CrossRef](#)]
140. Liang, R.; Dai, K.; Shi, X.; Guo, B.; Dong, X.; Liang, F.; Tomás, R.; Wen, N.; Fan, X. Automated Mapping of Ms 7.0 Jiuzhaigou Earthquake (China) Post-Disaster Landslides Based on High-Resolution UAV Imagery. *Remote Sens.* **2021**, *13*, 1330. [[CrossRef](#)]
141. Sukplum, W.; Wannawongsa, S. Massive Sandstone Falling Analysis and Design Barriers Along National Highway No. 2013 in Phitsanulok Province, Thailand: A Case Study. *Indian Geotech. J.* **2022**, *52*, 742–752. [[CrossRef](#)]
142. Kumar, N.S.; Ismail, M.A.M.; Sukor, N.S.A.; Cheang, W. Geohazard reconnaissance mapping for potential rock boulder fall using low altitude UAV photogrammetry. *IOP Conf. Ser. Mater. Sci. Eng.* **2017**, *352*, 012033. [[CrossRef](#)]
143. Gailler, L.; Labazuy, P.; Régis, E.; Bontemps, M.; Souriot, T.; Bacques, G.; Carton, B. Validation of a New UAV Magnetic Prospecting Tool for Volcano Monitoring and Geohazard Assessment. *Remote Sens.* **2021**, *13*, 894. [[CrossRef](#)]
144. Derrien, A.; Villeneuve, N.; Peltier, A.; Beauducel, F. Retrieving 65 years of volcano summit deformation from multitemporal structure from motion: The case of Piton de la Fournaise (La Réunion Island). *Geophys. Res. Lett.* **2015**, *42*, 6959–6966. [[CrossRef](#)]
145. Gracchi, T.; Tacconi Stefanelli, C.; Rossi, G.; Di Traglia, F.; Nolesini, T.; Tanteri, L.; Casagli, N. UAV-Based Multitemporal Remote Sensing Surveys of Volcano Unstable Flanks: A Case Study from Stromboli. *Remote Sens.* **2022**, *14*, 2489. [[CrossRef](#)]
146. Santagata, T. Monitoring of the Nirano Mud Volcanoes Regional Natural Reserve (North Italy) using Unmanned Aerial Vehicles and Terrestrial Laser Scanning. *J. Imaging* **2017**, *3*, 42. [[CrossRef](#)]
147. Gomez, C.; Setiawan, M.A.; Listyaningrum, N.; Wibowo, S.B.; Hadmoko, D.S.; Suryanto, W.; Darmawan, H.; Bradak, B.; Daikai, R.; Sunardi, S.; et al. LiDAR and UAV SfM-MVS of Merapi Volcanic Dome and Crater Rim Change from 2012 to 2014. *Remote Sens.* **2022**, *14*, 5193. [[CrossRef](#)]
148. Beselly, S.M.; van der Wegen, M.; Grueters, U.; Reyns, J.; Dijkstra, J.; Roelvink, D. Eleven Years of Mangrove–Mudflat Dynamics on the Mud Volcano-Induced Prograding Delta in East Java, Indonesia: Integrating UAV and Satellite Imagery. *Remote Sens.* **2021**, *13*, 1084. [[CrossRef](#)]
149. Rokhmana, C.A.; Andaru, R. Utilizing UAV-based mapping in post disaster volcano eruption. In Proceedings of the 2016 6th International Annual Engineering Seminar (InAES), Yogyakarta, Indonesia, 1–3 August 2016; pp. 202–205. [[CrossRef](#)]
150. Yaprak, S.; Yildirim, Ö.; Susam, T. UAV Based Agricultural Planning and Landslide Monitoring. *TeMA-J. Land Use Mobil. Environ.* **2017**, *10*, 325–338. [[CrossRef](#)]
151. Kyriou, A.; Nikolakopoulos, K.; Koukouvelas, I.; Lampropoulou, P. Repeated UAV Campaigns, GNSS Measurements, GIS, and Petrographic Analyses for Landslide Mapping and Monitoring. *Minerals* **2021**, *11*, 300. [[CrossRef](#)]
152. Jovančević, S.D.; Peranić, J.; Ružić, I.; Arbanas, Ž. Analysis of a historical landslide in the Rječina River Valley, Croatia. *Geoenviron. Disasters* **2016**, *3*, 26. [[CrossRef](#)]
153. Gantimurova, S.; Parshin, A.; Erofeev, V. GIS-Based Landslide Susceptibility Mapping of the Circum-Baikal Railway in Russia Using UAV Data. *Remote Sens.* **2021**, *13*, 3629. [[CrossRef](#)]
154. Peppas, M.V.; Mills, J.P.; Moore, P.; Miller, P.E.; Chambers, J.E. Brief communication: Landslide motion from cross correlation of UAS-derived morphological attributes. *Nat. Hazards Earth Syst. Sci.* **2017**, *17*, 2143–2150. [[CrossRef](#)]
155. Rossi, G.; Tanteri, L.; Tofani, V.; Vannocci, P. Multitemporal UAV surveys for landslide mapping and characterization. *Landslides* **2018**, *15*, 1045. [[CrossRef](#)]
156. Rau, J.Y.; Jhan, J.P.; Lo, C.F.; Lin, Y.S. Landslide mapping using imagery acquired by a fixed-wing UAV. *Int. Arch. Photogramm. Remote Sens. Spat. Inf. Sci.* **2011**, *38/1-C22*, 195–200. [[CrossRef](#)]
157. Migliazza, M.; Carriero, M.T.; Lingua, A.; Pontoglio, E.; Scavia, C. Rock Mass Characterization by UAV and Close-Range Photogrammetry: A Multiscale Approach Applied along the Vallone dell’Elva Road (Italy). *Geosciences* **2021**, *11*, 436. [[CrossRef](#)]
158. Xu, Q.; Ye, Z.; Liu, Q.; Dong, X.; Li, W.; Fang, S.; Guo, C. 3D Rock Structure Digital Characterization Using Airborne LiDAR and Unmanned Aerial Vehicle Techniques for Stability Analysis of a Blocky Rock Mass Slope. *Remote Sens.* **2022**, *14*, 3044. [[CrossRef](#)]
159. Car, M.; Kačunić, D.J.; Kovačević, M.S. Application of Unmanned Aerial Vehicle for Landslide Mapping. In Proceedings of the International Symposium on Engineering Geodesy—SIG 2016, Varaždin, Croatia, 20–22 May 2016; pp. 549–559.
160. Kovacevic, M.S.; Car, M.; Bacic, M.; Stipanovic, I.; Gavin, K.; Noren-Cosgriff, K.; Kaynia, A. *Report on the Use of Remote Monitoring for Slope Stability Assessments; H2020-MG 2014-2015; Innovations and Networks Executive Agency: Zagreb, Croatia, 2015.*
161. Junaid, M.; Abdullah, R.A.; Sa’ari, R.; Rehman, H.; Shah, K.S.; Ullah, R.; Alel, M.N.A.; Zainal, I.Z.; Zainuddin, N.E. Quantification of Rock Mass Condition Based on Fracture Frequency Using Unmanned Aerial Vehicle Survey for Slope Stability Assessment. *J. Indian Soc. Remote Sens.* **2022**, *50*, 2041–2054. [[CrossRef](#)]
162. Štroner, M.; Urban, R.; Kremen, T.; Braun, J. UAV DTM Acquisition in a Forested Area—Comparison of Low-Cost Photogrammetry (DJI Zenmuse P1) and LiDAR Solutions (DJI Zenmuse L1). *Eur. J. Remote Sens.* **2023**, *56*, 2179942. [[CrossRef](#)]
163. Vemulapalli, S.C.; Mesapam, S. Slope Stability Analysis for Mine Hazard Assessment Using UAV. *J. Indian Soc. Remote Sens.* **2021**, *49*, 1483–1491. [[CrossRef](#)]

164. Blišťan, P.; Kovanič, L.; Zelizňaková, V.; Palková, J. Using UAS photogrammetry to document rock outcrops. *Acta Montan. Slovaca* **2016**, *21*, 154–161.
165. Giordan, D.; Adams, M.S.; Aicardi, I.; Alicandro, M.; Allasia, P.; Baldo, M.; De Berardinis, P.; Dominici, D.; Godone, D.; Hobbs, P.; et al. The use of unmanned aerial vehicles (UAVs) for engineering geology applications. *Bull. Eng. Geol. Environ.* **2020**, *79*, 3437–3481. [[CrossRef](#)]
166. Tziavou, O.; Pytharouli, S.; Souter, J. Unmanned aerial vehicle (UAV) based mapping in engineering geological surveys: Considerations for optimum results. *Eng. Geol.* **2018**, *232*, 12–21. [[CrossRef](#)]
167. Bemis, S.P.; Micklethwaite, S.; Turner, D.; James, M.R.; Akciz, S.; Thiele, S.T.; Bangash, H.A. Ground-based and UAV-Based photogrammetry: A multi-scale, high-resolution mapping tool for structural geology and paleoseismology. *J. Struct. Geol.* **2014**, *69*, 163–178. [[CrossRef](#)]
168. Nesbit, P.R.; Durkin, P.R.; Hugenholtz, C.H.; Hubbard, S.M.; Kucharczyk, M. 3-D stratigraphic mapping using a digital outcrop model derived from UAV images and structure-from-motion photogrammetry. *Geosphere* **2018**, *14*, 2469–2486. [[CrossRef](#)]
169. Dering, G.M.; Micklethwaite, S.; Thiele, S.T.; Vollgger, S.A.; Cruden, A.R. Review of drones, photogrammetry and emerging sensor technology for the study of dykes: Best practises and future potential. *JVGR* **2019**, *373*, 148–166. [[CrossRef](#)]
170. Ružič, I.; Benac, Č.; Jovančević, S.D.; Radišić, M. The Application of UAV for the Analysis of Geological Hazard in Krk Island, Croatia, Mediterranean Sea. *Remote Sens.* **2021**, *13*, 1790. [[CrossRef](#)]
171. Tauro, F.; Selker, J.; van de Giesen, N.; Abrate, T.; Uijlenhoet, R.; Porfiri, M.; Manfreda, S.; Caylor, K.; Moramarco, T.; Benveniste, J.; et al. Measurements and Observations in the XXI century (MOXXI): Innovation and multi-disciplinarity to sense the hydrological cycle. *Hydrol. Sci. J.* **2018**, *63*, 169–196. [[CrossRef](#)]
172. Manfreda, S.; McCabe, M.F.; Miller, P.E.; Lucas, R.; Pajuelo Madrigal, V.; Mallinis, G.; Ben Dor, E.; Helman, D.; Estes, L.; Ciruolo, G.; et al. On the Use of Unmanned Aerial Systems for Environmental Monitoring. *Remote Sens.* **2018**, *10*, 641. [[CrossRef](#)]
173. Höfle, B.; Vetter, M.; Pfeifer, N.; Mandlbürger, G.; Stötter, J. Water surface mapping from airborne laser scanning using signal intensity and elevation data. *Earth Surf. Process. Landf.* **2009**, *34*, 1635–1649. [[CrossRef](#)]
174. Mandlbürger, G.; Pfennigbauer, M.; Wieser, M.; Riegl, U.; Pfeifer, N. Evaluation of a novel UAV-borne topo-bathymetric laser profiler. *Int. Arch. Photogramm. Remote Sens. Spat. Inf. Sci.* **2016**, *XLI-B1*, 933–939. [[CrossRef](#)]
175. Huang, W.-C.; Young, C.-C.; Liu, W.-C. Application of an Automated Discharge Imaging System and LSPIV during Typhoon Events in Taiwan. *Water* **2018**, *10*, 280. [[CrossRef](#)]
176. Langhammer, J. UAV Monitoring of Stream Restorations. *Hydrology* **2019**, *6*, 29. [[CrossRef](#)]
177. Watanabe, Y.; Kawahara, Y. UAV photogrammetry for monitoring changes in river topography and vegetation. *Procedia Eng.* **2016**, *154*, 317–325. [[CrossRef](#)]
178. Flener, C.; Vaaja, M.; Jaakkola, A.; Krooks, A.; Kaartinen, H.; Kukko, A.; Kasvi, E.; Hyypä, H.; Hyypä, J.; Alho, P. Seamless Mapping of River Channels at High Resolution Using Mobile LiDAR and UAV-Photography. *Remote Sens.* **2013**, *5*, 6382–6407. [[CrossRef](#)]
179. Kameyama, S.; Sugiura, K. Estimating Tree Height and Volume Using Unmanned Aerial Vehicle Photography and SfM Technology, with Verification of Result Accuracy. *Drones* **2020**, *4*, 19. [[CrossRef](#)]
180. Zhang, R.; Li, H.; Duan, K.; You, S.; Liu, K.; Wang, F.; Hu, Y. Automatic Detection of Earthquake-Damaged Buildings by Integrating UAV Oblique Photography and Infrared Thermal Imaging. *Remote Sens.* **2020**, *12*, 2621. [[CrossRef](#)]
181. Marčič, M.; Fraštia, M.; Hideghéty, A.; Paulík, P. Videogrammetric Verification of Accuracy of Wearable Sensors Used in Kiteboarding. *Sensors* **2021**, *21*, 8353. [[CrossRef](#)] [[PubMed](#)]
182. Kalacska, M.; Arroyo-Mora, J.P.; De Gea, J.; Snirer, E.; Herzog, C.; Moore, T.R. Videographic Analysis of *Eriophorum Vaginatatum* Spatial Coverage in an Ombotrophic Bog. *Remote Sens.* **2013**, *5*, 6501–6512. [[CrossRef](#)]
183. Borowik, G.; Koźdoń-Debecka, M.; Strzelecki, S. Mutable Observation Used by Television Drone Pilots: Efficiency of Aerial Filming Regarding the Quality of Completed Shots. *Electronics* **2022**, *11*, 3881. [[CrossRef](#)]
184. Karakostas, I.; Mademlis, I.; Nikolaidis, N.; Pitas, I. Shot type constraints in UAV cinematography for autonomous target tracking. *Inf. Sci.* **2020**, *506*, 273–294. [[CrossRef](#)]
185. Pecho, P.; Hruz, M.; Skvarekova, I.; Azaltovic, V. Optimization of Persons Localization Using a Thermal Imaging Scanner Attached to UAV. In Proceedings of the 2020 New Trends in Aviation Development (NTAD), Starý Smokovec, Slovakia, 17–18 September 2020. [[CrossRef](#)]
186. Sun, J.; Li, B.; Jiang, Y.; Wen, C.-y. A Camera-Based Target Detection and Positioning UAV System for Search and Rescue (SAR) Purposes. *Sensors* **2016**, *16*, 1778. [[CrossRef](#)] [[PubMed](#)]
187. Zimroz, P.; Trybała, P.; Wróblewski, A.; Góralczyk, M.; Szrek, J.; Wójcik, A.; Zimroz, R. Application of UAV in Search and Rescue Actions in Underground Mine—A Specific Sound Detection in Noisy Acoustic Signal. *Energies* **2021**, *14*, 3725. [[CrossRef](#)]
188. Lygouras, E.; Santavas, N.; Taitzoglou, A.; Tarchanidis, K.; Mitropoulos, A.; Gasteratos, A. Unsupervised Human Detection with an Embedded Vision System on a Fully Autonomous UAV for Search and Rescue Operations. *Sensors* **2019**, *19*, 3542. [[CrossRef](#)] [[PubMed](#)]
189. Masný, M.; Weis, K.; Biskupič, M. Application of Fixed-Wing UAV-Based Photogrammetry Data for Snow Depth Mapping in Alpine Conditions. *Drones* **2021**, *5*, 114. [[CrossRef](#)]
190. Liu, C.; Szirányi, T. Road Condition Detection and Emergency Rescue Recognition Using On-Board UAV in the Wildness. *Remote Sens.* **2022**, *14*, 4355. [[CrossRef](#)]

191. Cho, S.-W.; Park, J.-H.; Park, H.-J.; Kim, S. Multi-UAV Coverage Path Planning Based on Hexagonal Grid Decomposition in Maritime Search and Rescue. *Mathematics* **2022**, *10*, 83. [[CrossRef](#)]
192. Utsav, A.; Abhishek, A.; Suraj, P.; Badhai, R.K. An IoT Based UAV Network For Military Applications. In Proceedings of the 2021 Sixth International Conference on Wireless Communications, Signal Processing and Networking (WiSPNET), Chennai, India, 25–27 March 2021; pp. 122–125. [[CrossRef](#)]
193. Ko, Y.; Kim, J.; Duguma, D.G.; Astillo, P.V.; You, I.; Pau, G. Drone Secure Communication Protocol for Future Sensitive Applications in Military Zone. *Sensors* **2021**, *21*, 2057. [[CrossRef](#)]
194. Xiaoning, Z. Analysis of military application of UAV swarm technology. In Proceedings of the 2020 3rd International Conference on Unmanned Systems (ICUS), Harbin, China, 27–28 November 2020; pp. 1200–1204. [[CrossRef](#)]
195. Jiang, Y.; Mi, Z.; Wang, H. An Improved OLSR Protocol Based on Task Driven Used for Military UAV Swarm Network. In *Intelligent Robotics and Applications*; Yu, H., Liu, J., Liu, L., Ju, Z., Liu, Y., Zhou, D., Eds.; ICIRA 2019. Lecture Notes in Computer Science; Springer: Cham, Switzerland, 2019; Volume 11742. [[CrossRef](#)]
196. Ma'sum, A.M.; Arrofi, M.K.; Jati, G.; Arifin, F.; Kurniawan, M.N.; Mursanto, P.; Jatmiko, W. Simulation of intelligent Unmanned Aerial Vehicle (UAV) For military surveillance. In Proceedings of the International Conference on Advanced Computer Science and Information Systems (ICACSIS), Sanur Bali, Indonesia, 28–29 September 2013; Volume 2013, pp. 161–166. [[CrossRef](#)]
197. Zhang, M.; Li, H.; Xia, G.; Zhao, W.; Ren, S.; Wang, C. Research on the Application of Deep Learning Target Detection of Engineering Vehicles in the Patrol and Inspection for Military Optical Cable Lines by UAV. In Proceedings of the 2018 11th International Symposium on Computational Intelligence and Design (ISCID), Hangzhou, China, 8–9 December 2018; pp. 97–101. [[CrossRef](#)]
198. Bao, W.; Ren, Y.; Wang, N.; Hu, G.; Yang, X. Detection of Abnormal Vibration Dampers on Transmission Lines in UAV Remote Sensing Images with PMA-YOLO. *Remote Sens.* **2021**, *13*, 4134. [[CrossRef](#)]
199. Zhang, Y.; Yuan, X.; Fang, Y.; Chen, S. UAV Low Altitude Photogrammetry for Power Line Inspection. *ISPRS Int. J. Geo-Inf.* **2017**, *6*, 14. [[CrossRef](#)]
200. Kuhnert, K.-D.; Kuhnert, L. Light-weight sensor package for precision 3d measurement with micro UAVs eg power-line monitoring. *ISPRS-Int. Arch. Photogramm. Remote Sens. Spat. Inf. Sci.* **2013**, *XL-1/W2*, 235–240. [[CrossRef](#)]
201. Liu, C.; Liu, Y.; Wu, H.; Dong, R. A Safe Flight Approach of the UAV in the Electrical Line Inspection. *Int. J. Emerg. Electr. Power Syst.* **2015**, *16*, 503–515. [[CrossRef](#)]
202. Chang, A.; Liang, Y.; Jiang, M.; Li, X.; Chen, Z.; Liu, R. Application of UAV Intelligent Management and Control Platform on Overhead Transmission Lines Inspection. In *Forthcoming Networks and Sustainability in the IoT Era*; Al-Turjman, F., Rasheed, J., Eds.; FoNeS-IoT 2021. Lecture Notes on Data Engineering and Communications Technologies; Springer: Cham, Switzerland, 2022; Volume 130. [[CrossRef](#)]
203. Cantieri, A.R.; Wehrmeister, M.A.; Oliveira, A.S.; Lima, J.; Ferraz, M.; Szekir, G. Proposal of an Augmented Reality Tag UAV Positioning System for Power Line Tower Inspection. In Proceedings of the Robot 2019: Fourth Iberian Robotics Conference, Porto, Portugal, 20–22 November 2019; Silva, M., Luís Lima, J., Reis, L., Sanfeliu, A., Tardioli, D., Eds.; ROBOT 2019. Advances in Intelligent Systems and Computing. Springer: Cham, Switzerland, 2020; Volume 1092. [[CrossRef](#)]
204. Shi, J.-G.; Miao, W.; Si, H. Visualization and Analysis of Mapping Knowledge Domain of Urban Vitality Research. *Sustainability* **2019**, *11*, 988. [[CrossRef](#)]
205. Granshaw, S.I. Photogrammetric Terminology: Fourth Edition. *Photogramm. Rec.* **2020**, *35*, 143–288. [[CrossRef](#)]

**Disclaimer/Publisher's Note:** The statements, opinions and data contained in all publications are solely those of the individual author(s) and contributor(s) and not of MDPI and/or the editor(s). MDPI and/or the editor(s) disclaim responsibility for any injury to people or property resulting from any ideas, methods, instructions or products referred to in the content.